Biomimetic Design of Poly(ether ether ketone) Composites for Bone Replacement

Christopher D. Rader

Thesis submitted to the faculty of the Virginia Polytechnic Institute and State University in partial fulfillment of the requirements for the degree of

Master of Science
In
Materials Science and Engineering

Johan E. Foster
Hervé Marand
Robert Moore

October 11, 2017
Blacksburg, VA

Keywords: Biomedical, Composite processing, Material properties

Biomimetic Design of Poly(ether ether ketone) Composites for Bone Replacement

Christopher D. Rader

ABSTRACT

Hip and knee replacements are a common solution for patients whom have experienced loss in knee cartilage or have fractured their bones due to the weakening of the bone from osteoporosis. The number of bone replacements continues to rise as the number of ACL and meniscus repair surgeries increases. These surgeries accelerate the loss of cartilage especially at the knee. Current materials in use are nickel-cobalt alloys, titanium, and high-density polyethylene. These replacements have a lifespan of 10-20 years with a 10% risk of rejection from the body. Rejection can be caused by metal leeching into the bloodstream, growth of bacteria on the surface of the material, and the weakening of bone at the interface due to a large difference in young's modulus between the replacement material and bone. Additionally, today's bone replacement does not replicate the porous structure of bone to allow for the growth of bone cells. This research expands on a potential new material for bone replacement, poly(ether ether ketone) or PEEK. PEEK is a polymer that can be introduced to the body without rejection, and has been used as a material for spinal fusions and partial skull replacements. Additionally, not being a metal, PEEK avoids the risk of the introduction of metals into the bloodstream and weakening of surrounding bone due to its young's modulus being lower than bone. However, traditional processing methods of injection or compression molding require high heat for melt resulting in a restriction of the structure and narrowing additives to inorganics. We introduce a unique solvent casting process with the use of chlorophenol dissolving PEEK at 150 °C. The process varies average pore sizes and allows for the introduction of organic and inorganic additives, cellulose nanocrystals and hydroxyapatite, to change the mechanical properties as well as provide a foundation for bone cell growth. We analyze the properties of the PEEK and PEEK composites through SEM imaging, thermal analysis, and mechanical testing. SEM imaging displays pore sizes in the nanometer ranges which are too small for cellular growth but small enough for mineralization. Thermogravimetric analysis confirms a proper distribution of additives within the PEEK. From differential scanning calorimetry, residual solvent remains from the processing. For mechanical testing, the additives' significance on the PEEK composites could not be determined. However, evidence points towards higher drying temperatures, for solvent removal, increasing the modulus and yield strength of the PEEK and PEEK composites. Future research should be conducted to increase the pore size to allow for cell growth as well as cell culture studies to look at the degree of cell growth on the samples. Also, experiments should be performed to fully remove solvents and the understand the effect of drying temperatures on the PEEK composites' structure and properties.

Biomimetic Design of Poly(ether ether ketone) Composites for Bone Replacement

Christopher D. Rader

GENERAL AUDIENCE ABSTRACT

Hip and knee replacements are a common solution for patients whom have experienced loss in knee cartilage or have fractured their bones. According to the American Joint Replacement Registry, close to 400,000 total hip and knee replacement procedures were conducted in 2016 with an 100% increase from the previous year. The number of bone replacements continues to rise as the number of knee ligament and meniscus repair surgeries increases. These repairs accelerate the loss of cartilage at the knee due to an imbalance within the joint. At extreme conditions of ligament and meniscus damage, a total bone replacement is needed. These replacements remove all ligaments and rely on the replacement material to provide stability in all directions. Because of the lack of ligaments, movement is restricted to bending motions. Current materials to replace bone are metals such as titanium or polymers such as polyethylene. These replacements have an estimated lifespan of 10-20 years with a 10% risk of rejection from the body. Rejection can be caused by metal leeching into the bloodstream, growth of bacteria on the surface of the material, and the weakening of bone at the interface. Additionally, today's bone replacement does not replicate the porous structure of bone to allow for the growth of bone cells. This research expands on a potential new material, with a new process method, for bone replacement, poly(ether ether ketone) or PEEK. PEEK is a polymer that can be introduced to the body without rejection, and has been used as a material for spinal fusions and partial skull replacements. Additionally, not being a metal, PEEK avoids the risk of the introduction of metals into the bloodstream and weakening of surrounding bone. However, traditional melt processing methods restrict the structure and composition of PEEK. We introduce a solvent casting process that avoids melting the PEEK at high temperatures. The process alters the structure of PEEK, thus moving towards mimicking the structure of bone. To replicate bone further and increase strength, hydroxyapatite and cellulose nanocrystals are added to develop nanocomposites. Imaging shows the introduction of pores into PEEK depending on the drying conditions. These pores are too small for cell growth but small enough for the mineralization of bone. Thermal analysis exhibits a distribution of the additives with no alteration of the PEEK's thermal stability from the process. From mechanical tests, the PEEK composites are weaker than that of bone. Future research should be conducted to increase the pore size to allow for cell growth as well as cell culture studies to look at the degree of cell growth on the samples.

Acknowledgements

First, I want to thank my parents for always being the basis of my motivation. I would like to acknowledge my research group for helping make this project and thesis come to fruition. I would especially like to acknowledge my advisor, Dr. Johan Foster, for guiding me in this project from day one. I would also like to thank my defense committee for the insight and wisdom they have given along the course of this project.

Table of Contents

1 Goals and Motives

Today, hip and knee replacements are a common solution for fractured femurs and tibias, or patients with a high degree of osteoarthritis. With increasing age, the risk of fracturing one's bone increases due to the deterioration of spongy and cortical bone known as osteoporosis. An imbalance of bone cell repair and cleaning results in the body removing more bone than it is replacing. Causes of osteoporosis are low levels of testosterone and estrogen as well as low physical activity. Because of this, it has been recorded that 450,000 knee and hip replacement surgeries are conducted annually. [15] Coupled with osteoporosis, osteoarthritis contributes to the need for bone replacements. Osteoarthritis is the degradation of the cartilage at the joint leading to pain due to inflammation, instability of the joint, and bone on bone grinding. At the knee, repair of the cartilage and surrounding ligaments expedites the progression of osteoarthritis, thus increasing the demand for knee replacements. Reconstruction of the cartilage and ligaments puts additional stress on the knee. ACL tears couple with meniscal tears because of the loss of lateral stability in the knee; therefore, the same surgery repairs both components. [16] Meniscal repair surgery removes portions of the cartilage in order to provide a smooth contact surface. There is no replacement for the removed cartilage leading to a thinner layer of cartilage to protect and bear load at the joint. Due to ligament and meniscus reconstruction, the number of joint replacements for people in their 40s has increased due to early injuries. [10] By 2030 the number of annual knee and hip replacements is to increase by 500%. [15] Unfortunately with the rising demand of bone replacements, current replacement materials have a 9-10% chance of rejection with an average lifetime of 10-20 years. [17-18] Leading causes of rejection correlate to the use of metals such as titanium, cobalt, and nickel. These metals have strength values greater than human body causing a degradation in the surrounding bone tissue known as bone shielding. [19-21] On top of the difference in strength, the corrosion of the metal, known as ion leaching or metallosis, insights inflammation and the body begins to fight the replacement like an infection. The release of metal ions into the body is a result of low wear resistance in metal-metal or metal-polymer contact surfaces. At the joints, replacements consist of metal-polymer composites to prevent metal on metal wearing. For replacements within the bone, metals are common due to the lack of the grinding. Ceramic replacements, such as hydroxyapatite, are ideal because of their ability to promote bone growth, but ceramics lack toughness and are susceptible to abrupt, brittle fracture. Bone growth requires nutrients and a porous network for cells to grow into. To maintain their high strength, metal

replacements do not have the porous network. However, coupling metals and hydroxyapatite can improve the integration of the replacement with the surrounding bone.

The goal of this project is to look into a composite that replicates the structure of bone to house bone growth, and possesses mechanical properties in range of bone to prevent bone shielding Looking closely at the structure of today's bone replacements, the materials are bulk and dense. Although the materials have the mechanical properties good for bearing loads, the structure does not match bone. The dense structures do not allow for the growth of bone cells in order to improve the osteointegration of the implant. Poly(ether ether ketone) or PEEK shows promise owing to its high wear resistance, high strength to weight ratio, and biocompatibility. [21-23] A solvent exchange process develops a porous structure of PEEK. A PEEK composite with the introduction of fillers, such as cellulose nanocrystals or hydroxyapatite, can be made with a structure similar to bone for osteointegration. Cellulose nanocrystals are known to increase the mechanical properties of polymers through proper distribution. [24-26] Additionally adding phosphate groups to the cellulose nanocrystals invokes hydroxyapatite growth further increasing osteointegration. [27] With a solvent casting process, a PEEK composite with the addition of hydroxyapatite and cellulose nanocrystals provides a foundation for a material to replace bone.

2 Introduction

2.1 Human Bone Anatomy

2.1.1 Flat

Examples of flat bone can be seen in the skull, scapula, and rib cage. Their structure incorporates two thin layers of cortical bone separated by cancellous bone creating a sandwich structure. [20] The thin wall structure's main function is for the protection of vital organs. Additionally, the thin wall structure aids in the production of blood cells for the body through the bone marrow. [20] Bone marrow provides nutrients to the body and aids in the production of blood cells. Unique to long bones, which contains majority of the marrow in the center, bone marrow is distributed throughout the entirety of flat bones. Because of the even distribution of marrow, the gradient of porosity from the cancellous bone section to cortical bone is non-existent as increased porosity is correlated to increased marrow density. [20] A gradient in porosity in long bones is essential as the cancellous bone acts to withstand different amounts of load depending on the location. For example, the head of the femur, near the hip joint, contains a low porosity cancellous

bone as the need for load distribution is greater and bone marrow is not housed there. For flat bone, the cancellous bone's porosity is consistent throughout the structure to keep the strength consistent. [2, 20] The consistency in structure allows for flat bone to withstand impacts and distribute loads in all directions. Unlike long bones, which are structured for withstanding longitudinal loads, flat bones' structure develops an isotropic material with the same strength in bending, compression, and tension. With flat bone's function to protect vital organs, a sandwich structure is seen to provide protection for forces in all directions.

2.1.2 Short

Short bones are found in the ankles and wrist. Compared to the other bone types, the length of short bones is equal to their width. With their location being at the joints, the main function is to provide joint stability as well as be resistant to movement. Additionally, their small size and block shape make them optimal for compressive loads with little bending. [20] In terms of blood cell production and bone marrow content, short bones do not contain bone marrow.

2.1.3 Long

Long bones are the main focus of bone replacement. More specifically, the sections of the long bone near the joints, so the ends of the femur near the hip and knee. These areas withstand the majority of damage from day to day activities, and are where osteoarthritis beings to develop. Additionally, with the task of bearing a majority of the body's load, the weakening of the bone through osteoporosis causes fractures. Bones such as the femur, tibia, humerus, and radius found in the legs and arms are categorized as long bones. As the name suggests, long bones contain a small width to length ratio. Their structure consists of cortical bone surrounding cancellous bone to develop a thin-walled cylinder with a higher concentration of cancellous bone at the joints. [20] An illustration for the gradient of cancellous and cortical bone can be seen in Figure (1). A porosity change exists in the femur head as the cancellous bone becomes less dense further away from the joint site. Cortical bone is an anisotropic material due to orientation of the cells; therefore, at the joint, cancellous bone is dominant to provide strength in all directions. Similar to flat bone, the cancellous bone section contains bone marrow, which supports the need for increased porosity. Interestingly, long bones' structure and development is to minimize mass and optimize mechanical strength by mimicking a thin-walled cylinder. [20] The cancellous bone and bone marrow act as the hollow or porous section, and the cortical bone being the thin wall holding in the cancellous bone.

Figure 1: Image of the head of the femur [8]

The porous section of long bone acts to provide support in all directions and prevent collapsing of the cortical bone. In this structure, the long bone is optimized to handle longitudinal loads, and the bending or shear stresses are absorbed by the cancellous bone and bone marrow. Thin-walled cylindrical structures are susceptible to buckling under large longitudinal loads. [28] The fluid in bone marrow acts to provide hydrostatic pressure preventing collapse of the surrounding cortical bone. [20] Overall, the thickness of the cortical bone wall is greatest for long bones to support longitudinal loads from walking and other physical activities. Because of the constant repetition of loads the long bones withstand, osteoarthritis development is common for long bone. Cyclic loading invokes the degradation of bone cells and cartilage at the joints. Over time, the repair of bone cells becomes irregular as more bone is removed while less is replaced. The uneven reconstruction of bone leaves a rough surface at the joint and concentrates stresses leading to osteoarthritis development. Long bones provide the structural support to handle loads experienced in daily movement, and are the focus for today's bone replacements.

2.2 Human Bone Layers

2.2.1 Periosteum

The outer layer of bone consists of periosteum. Periosteum does not consist of bone cells, but plays a vital role in the transport of nutrients in and out bone. Besides being the transport medium, periosteum provides the foundation for repairing damaged bone. [29-32] For long bones, the thickness of the periosteum layer thins at the joints. At the joints, the surface of the bone is attached to tendons and ligaments; thus, requiring less periosteum to allow attachment. [6] Cells that make

up the periosteum are dormant osteoblasts in a dense fibrous structure. Osteoblasts are the cells that produce collagenous matrix for later mineral growth in early stages of growth. [6, 20] During damage, the dormant osteoblasts are released to repair and replace damaged tissue. Figure (2) illustrates the layering and repairing system of the periosteum. The process of replacing damaged

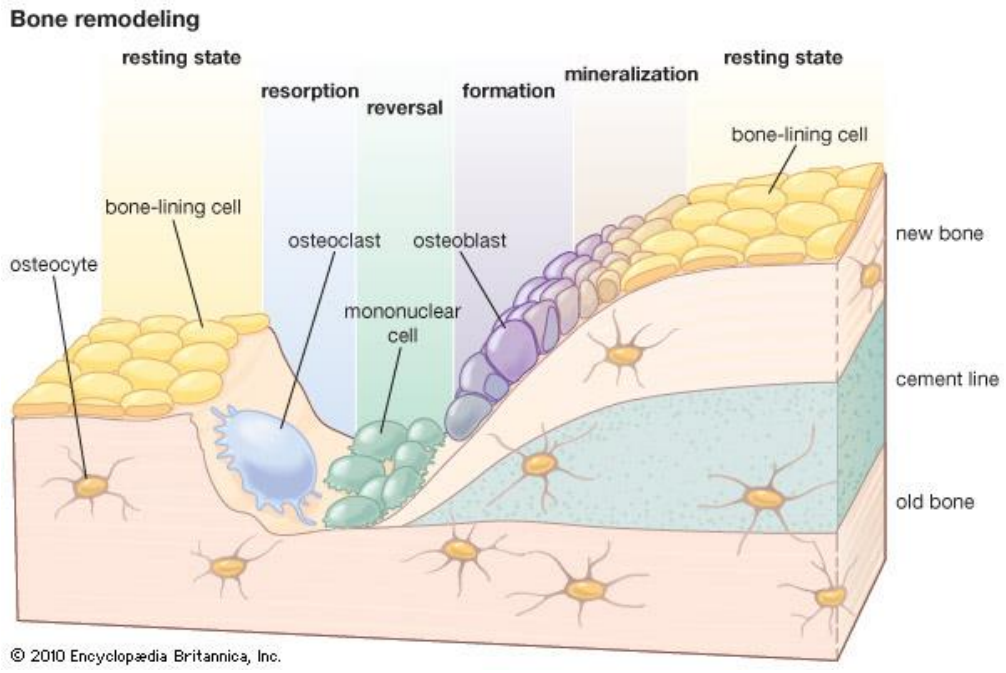

Figure 2: Bone remodeling diagram showing different layers of the periosteum [6]

bone is known as bone remodeling. [31] Bone remodeling occurs on a consistent basis due to the develop of microcracks from cyclic loads experienced daily. [31-32] Similar to replacing skin cells on a regular basis, bone is constantly replacing its old cells with new ones. The osteocytes act to absorb surrounding bone tissue and clean up damaged tissue. [30-31, 33] At the same time, the osteoblast that were once dormant begin to lay the foundation for bone formation which will later mineralize. The ratio between adsorption and formation is tightly regulated to keep rate of bone removed and replaced the same. Once the balance of adsorption and formation deviates with increasing adsorption of bone, early stages of osteoporosis become prevalent. [31] The osteoclasts tunnel through the old bone and with the lack of osteoblasts filling in the tunnels, the tunnels act as pores. [31] When left unchecked, the osteoclasts continue to tunnel through the bone layers increasing the porosity of the bone and decreasing the overall strength. For cancellous bone, the absorption from the osteoclasts happens a faster rate due to the high surface area. [34] Because of the high rate of absorption, the beginnings of osteoporosis start from the inner cancellous bone.

Additionally, the periosteum plays a vital role in transport of ions and nutrients from the body to the inner parts of the bone. [20, 30] With a network of blood vessels, the periosteum allows for blood cells from the marrow to be released into the rest of the body, while allowing nutrients to enter. As a semipermeable membrane, the direction and rate of flow in the periosteum has been studied to observe possible outside stresses changing the two factors. Interestingly at increased stress states, rate of flow from bone to muscle significantly overshadows that from muscle to bone. [30] A reason for the lob-sided flow rate is the release of nutrients and cells from the bone marrow is increased in states close to damage. [30] The change in permeability has caught interest in research groups to mimic the responsive nature of periosteum. Although lacking the support from loads, periosteum acts to repair bone and maintain nutrient transport.

2.2.2 Cortical

Cortical bone's role is to withstand loads in the human body. It consists of densely packed collagen fibers which are bundled together from the nano-scale up to the macro-scale. The fibers provide great tensile and compressive strength for axial loads, but not for bending loads. Cancellous bone protects against shear and bending loads. In the human skeletal system, cortical bone consists of 80% by volume of the bone with the remaining residing in cancellous bone and bone marrow. [34] Cortical bone consists of layers of lamella with little porosity. With a dense structure with porosity from 5-10%, cortical bone contains pores to allow for blood vessels and osteocytes to be present. [20, 35] From the nano to the macro scale, cortical bone is a composite of collagen fibers oriented and bundled together.[36] The collagen can be non-woven, but on the macroscale cortical bone displays a composite of cylindrical features known as the harversian structure. [36-38] Shown in Figure (3), the cylindrical shape of the bone formation can be seen. In the middle of the osteon or the center of the harversian system are small tubular channels that contain blood vessels and nerves. These blood vessels are essential in supplying nutrients to the surrounding bone cells such as the osteocytes for bone cell production. The cylindrical structure comes from the orientation of the lamellae surrounding the central canal. Important to note is that on a smaller scale the lamellae are a group of aligned collagen fibers oriented parallel to the blood vessels. Therefore, from the micro-scale to the macro-scale, cortical bone consists of cylindrical

shaped collagen fibers oriented in the longitudinal direction. Additionally, the lamellae contain minerals such as hydroxyapatite which give cortical bone its mechanical strength.

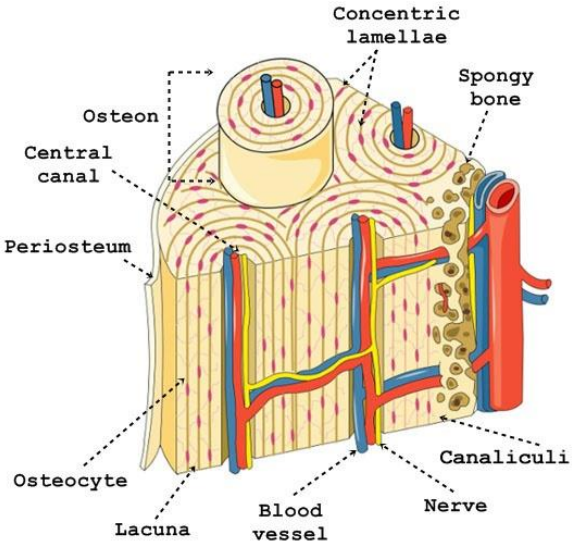

Figure 3: Structure of cortical bone known as the harversian system [14]

2.2.3 Cancellous

Cancellous or trabecular bone can be found in combination with cortical bone. Cancellous bone has a more porous structure compared to cortical while housing bone marrow. The main objectives of cancellous bone are to provide mechanical support against bending and shear, absorb energy, and house the nutrients needed to promote bone growth and repair. [20, 39] Unlike cortical bone, cancellous bone does not contain the harversian system of bone cells making cancellous bone an isotropic material. Looking at the image of a femur head in Figure (4), the difference in

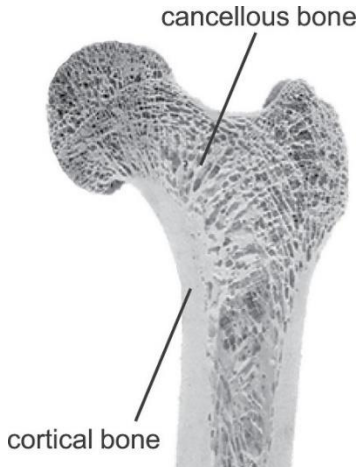

Figure 4: Image of femur head highlighting cancellous and cortical bone [5]

porosity can be seen between the cortical and cancellous bone. Furthermore, the concentration of cancellous bone is higher towards the head of the femur. As this is the part connected to the joint, the higher surface area distributes loads better. Although the cortical bone's harversian structure is optimized for withstanding loads, it is optimized in the direction of the fibers. Therefore, cancellous bone, being isotropic, can withstand forces at multiple angles, which is ideal for rotational movement at the joint. While cancellous bone handles forces in multiple directions, the cortical bone helps in distribution of forces down the entire length of the bone. [20, 40]

For mechanical properties, it is hard to separate data on cancellous bone from cortical bone as the two parts are always together in the human bone. The cancellous bone is encompassed by cortical bone in every bone type. Additionally, the degree of mineralization and hydration state determine the strength of the bone further complicating mechanical data on human bone. [8, 20] Elastic modulus in tension and ultimate tensile strength for the femur have been measured while the bone was in a wet state through ultrasonication methods. [8] In order to measure the mechanical properties, the bone is submerged in saline solution or water, and the change in the speed of sound is detected throughout the different tissue. [8, 20] In tension the femur's young's modulus, yield strength, and elongation at break were measured at 17 GPa, 124 MPa, and 1.41%. [8] In compression the young's modulus could not be measured through this method, but the yield strength and elongation at break are measured at 107 MPa and 1.85%. [8] From the ultrasonication methods, Figure (5) was developed to show a comparison in stress vs. strain to other common materials. Compared to steel and glass, bone showcases more ductility with a longer elongation at break and a lower yield point. However, samples tested through deformation in the Instron reveal much lower values in the mechanical properties. The young's modulus, tensile yield strength, and compressive

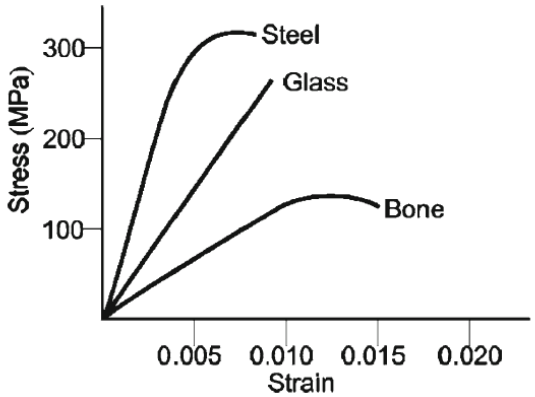

Figure 5: Stress vs. strain of steel, glass, and human bone [8]

yield strength registered at 338 MPa, 40 MPa, and 142 MPa. [41] Multiple factors affect the mechanical properties of bone such as history of damage through microcracks in the cortical and cancellous bone as well as freshness of the sample due to hydration and mineral content. Regardless, the conventional measurements of the mechanical properties of bone are through the ultrasonication of the tissue invitro. With that being said, testing for elasticity and strength in bone is best done while the bone cells are intact and in the right environment.

2.3 Bone Diseases and Damage

2.3.1 Osteoarthritis

Osteoarthritis is the degradation of the cartilage at the joints causing inflammation and pain. The degeneration of the cartilage creates an irregular surface leading to stiffness and slipping of the joint. The pain originates form a combination of continuous bone thickening at the joint and the wear of supporting cartilage. [4, 42] Figure (6) below illustrates the various stages of osteoarthritis seen in the knee. To judge the degree of osteoarthritis, radiographic imaging is performed on the joint in the form of MRIs and X-Ray. Initial stages of osteoarthritis involve the degeneration of cartilage or meniscus in the knee. At later stages the pain arises from bone on bone contact at the joint. The grinding and pounding between the two bones leads to microcracks and osteophyte

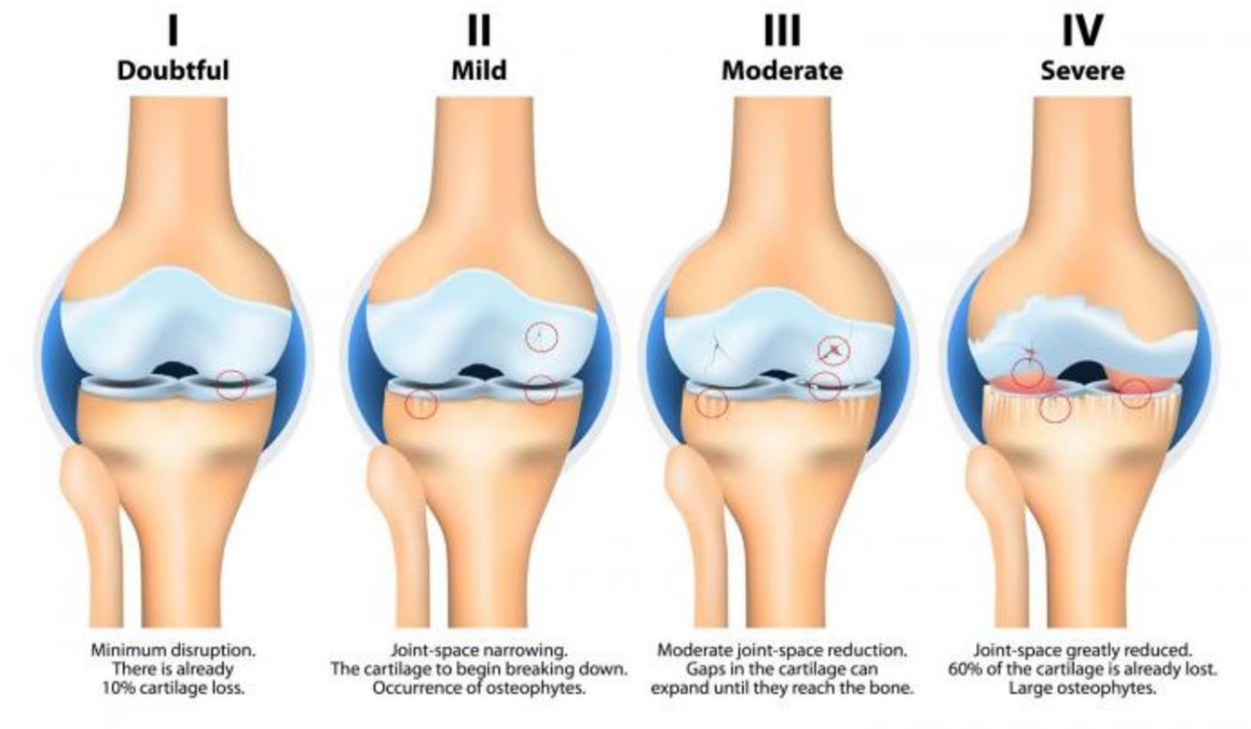

Figure 6: Stages of osteoarthritis in the knee [4]

growth. [10] In other words, the growth of bone and lack of cartilage generates a rough surface increasing the chance for slippage during movement and increased pain. Unfortunately, the chances of having osteoarthritis are high starting at age 65 due to natural degeneration of the cartilage after years of use. [42] Early age osteoarthritis has been documented and result from injuries at the joint, obesity, and other diseases such as gout. [4] In order to treat the cartilage damage from osteoarthritis, surgery to remove excess osteophytes[11], reshape cartilage[11], or a glucosamine supplement to improve joint lubrication[43] is given to patients.

2.3.1.1 Causes

Although osteoarthritis is common for people above the age of 65, joint injuries and reconstructive surgeries increase the risk of osteoarthritis at earlier ages. In a study done at John Hopkins University, those with anterior cruciate ligament (ACL) or meniscectomy surgeries have a 50% increased chance of developing osteoarthritis in the knee within 10-15 years of the surgery. [10] Figure (7) displays the trend in %OA or percentage of osteoarthritis detected in men and women

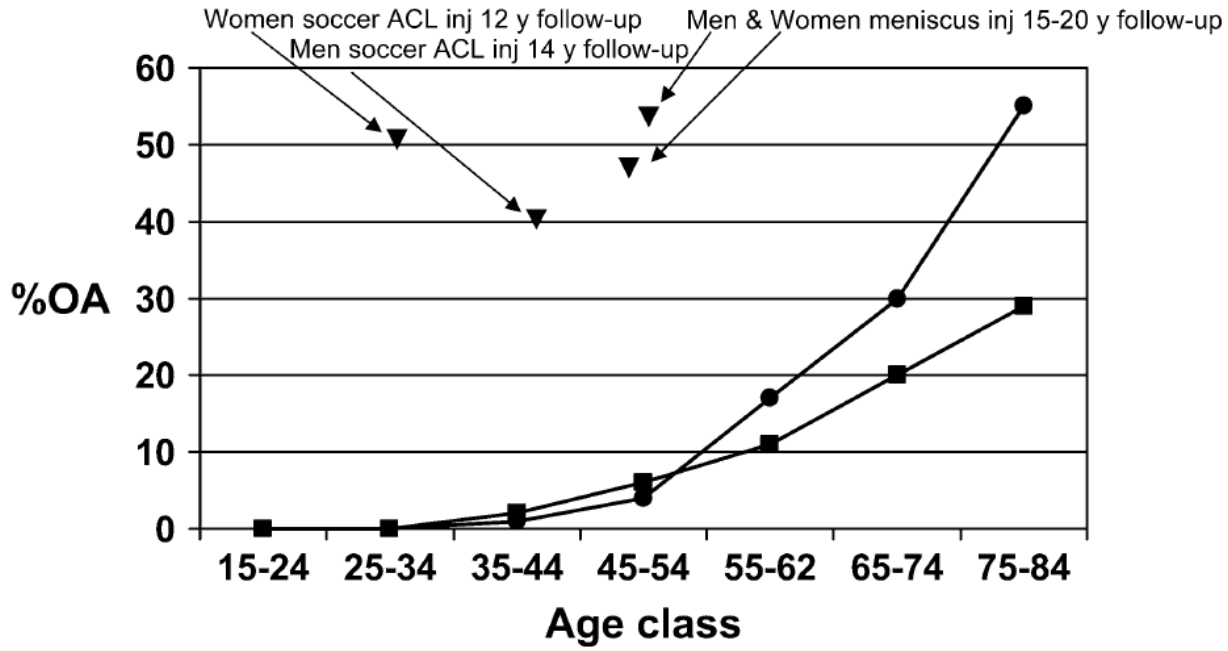

Figure 7: Plot comparing traditional trend In percentage of osteoarthritis vs. age compared to people with a history of knee surgeries. Controls groups illustrated with the circle (contralateral or injuried but not repaired knees) and squares (noninjuried knees) are used in comparison to knees that have undergone reconstructions [10]

after follow-ups from ACL reconstruction or meniscectomy. From surgery, multiple factors contribute towards osteoarthritis. For ACL reconstructions, the graft used to replace the ACL can be taken from different areas of the body. The patella tendon is a common graft as it as the ability to anchor into the tibia and femur for complete osteointegration. As a result, osteoarthritis develops

at the knee cap due to the shorter, tightened tendon. [10, 42] For aesthetic purposes, the hamstring tendon can be a replacement for an ACL. Although the hamstring tendon replacement does not have a revealing scar at the knee, the tendon's osteointegration is less than the patella. Compared to ACL reconstruction, the removal of the meniscus from a meniscectomy increases stress at the knee and reduces the load distribution, shock absorption, and joint stability. [10, 44] The rate of osteoarthritis is slower for a meniscus repair with radiographic features of osteoarthritis appearing 15 to 22 years earlier than the ACL reconstructions. [10, 44] Unfortunately, it is common to have a meniscus damage as a result of an ACL tear, so the factors of the two surgeries are coupled. Other than joint injuries, deconditioning of the musculoskeletal system instills osteoarthrosis development. [10] Sedentary lifestyles result in a lessening of muscle function, weight gain, and reduction of bone mass. [45] Proper muscle contraction is vital in distributing load at joints. [10, 45] Without repeated use of muscles, neuromuscular control weakens resulting in less efficient muscle contractions for movement and load bearing.[46-47] In regards to weight gain, the amplitude of the cyclic loading is greater at the joints; thus, accelerating the rate of wear on the cartilage. [10, 45] Lastly, a sedentary lifestyle does not promote densification of bone. Instead of promoting thickening of the bone to withstand higher loads, the bone walls thin due to a lack of loading as there is a lesser need for high load bearing. [48-49] Overall, the physiological causes of osteoarthritis from reconstruction develop a joint with poor load distribution.

Regardless of the cause of the onset of osteoarthritis the biological and biomechanics changes are similar. The function of a joint is to maintain stability between two bones. Cartilage is present at the joint to provide a smooth contact surface and to absorb cyclic compressive loads. [44, 50] Additionally, cartilage responds to loads by initiating growth in order to repair damaged tissue. [42, 50] Overtime, the cartilage begins to degenerate leading to a decrease in tensile strength and stiffness, and the rate of tissue repair slows down with age. [42] As the cartilage weakens, stress concentrations begin to develop within the cartilage matrix, and the spacing between the two bones narrows. [33] The stress concentrations create pathways for the bone to attempt to repair itself. [42, 48-49] Wolff's law describes the repairing of bone as a response to varying loads. The concept is the bone densifies as a response to increasing stresses this way the bone is more capable of withstanding these higher loads in the future. [49] In this process, the bones at the joint grow bone cells to adapt to the high loads at the stress concentrations. However, the uneven bone growth develops bone spurs; thus, changing the topography of the bone at the joint. [33] The rough surface

promotes slipping at the joint resulting further damage of the cartilage. At late stages of osteoarthritis, patients begin to experience stiffness and increased difficulty moving without severe pain. [4]

2.3.1.2 Treatment

Surgical means of repairs, although invasive, are necessary to repair and prevent further damage to the joint for patients at advanced stages of osteoarthritis. [51] In order to restructure the surface of the cartilage, cartilage repairs can be performed. For the knee, surgeries are performed to either reshape the cartilage or remove damaged cartilage. [11, 44] Reshaping of the cartilage is performed on younger patients to delay the onset of osteoarthritis. [11] This approach sounds counterintuitive, but the reshaping of cartilage is in part to increase load distribution. At younger ages, the rate of repair is higher; thus, making the reshaping option optimal in avoiding further development of osteoarthritis. Removal of cartilage is executed when the cartilage is perforated and to clean out dead tissue. [44] Unfortunately, this method is only available for joints in the hands, wrist, and knees. For the hip, total bone replacements are performed with materials such as titanium-polyethylene or ceramic-ceramic joints, when the severity of the osteoarthritis is high. [11, 51] For low levels of osteoarthritis, pain medication and physical therapy are utilized to lower inflammation and strengthen the surrounding muscles.[46] Other joints such as the wrist and ankle aren't replaced, but fusion surgeries are performed. Similar to total hip replacements, bone fusions at the wrists and ankles are last resort, because of the reduction of mobility at the joint. [11]

Without surgery, there are multiple ways to treat osteoarthritis through supplements to promote joint lubrication and physical therapy to improve biomechanics. For the knee, the quadricep can be developed to lessen the load on the cartilage within the joint. [10, 46-47] Additionally, the contraction of the quadricep while walking helps absorb shock. [10] Through physical therapy, osteoarthritis has been proven to decrease through development of surrounding muscle. Stretching, increases the range of motion at the joint, and increases neuromuscular connection for efficient muscle contractions. [46] An explanation for this improvement in load bearing can be balancing of biomechanics of the person resulting in restored load distribution at the joints. Another form of non-surgical treatment is supplementation. Bone morphogenic protein-7 has been utilized to protect cartilage after knee injuries. [52-53] The protein acts to reduce the degeneration of cartilage. However, the treatment works on early stages of osteoarthritis as it does not promote cartilage repair and growth. Additionally, glucosamine supplements have been used to prevent joint space

narrowing and lubricate the cartilage at the joints. [43] Another benefit of glucosamine is the ability to take the supplement orally without the need for onsite injections.

2.3.2 Osteoporosis

Osteoporosis is the rapid degeneration of bone tissue overtime. The cortical bone layer begins to thin and the cancellous bone begins to degrade leaving bone in a fragile state. Unfortunately, most people do not realize they have osteoporosis until a fracture occurs. [7] Figure (8) displays a schematic on the effects of osteoporosis. It can be seen that the cancellous bone tissue begins to degrade overtime. Over a long period of time, the cortical bone tissue becomes

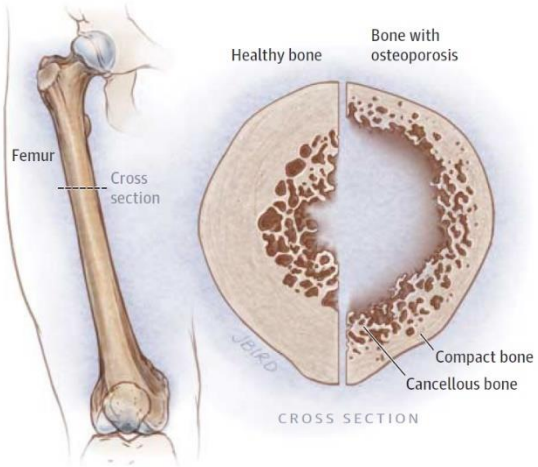

Figure 8: Schematic of the femur with evidence of osteoporosis [7]

more porous resembling that of cancellous bone. Referring back to the structure of bone, the thinning of the cortical bone wall reduces the ability for the bone to hold stress in the longitudinal direction. A reduction of cancellous bone mass lowers the bone's ability to handle shear and bending stress. Osteoporosis is a bone disease that alters the structure of bone reducing its mechanical properties; thus, making people susceptible to bone fracture.

2.3.2.1 Causes

Osteoporosis can occur based on primary and secondary causes. The primary cause is from aging, while secondary causes expedite bone loss and are factors from the environment such as alcohol abuse. Bone loss occurs naturally starting at age 40 known as osteopenia. The bone begins

to thin as the osteoblast activity begins to decline while osteoclast continues to operate at the same level. As a reminder, osteoclast clean out bone tissue to regulate blood calcium levels. They are vital in the remodeling and repair process for bones. Osteoblasts supply the hydroxyapatite required to promote bone growth. However, if the rate of bone loss is too rapid, osteoporosis occurs.

Osteoporosis is typically shown to start at the age of 65-70. The rate of bone loss varies slightly between men and women, but overall, the risks of osteoporosis are higher at older ages. The primary cause of osteoporosis is low levels of testosterone and estradiol also known as hypogonadism. [54-55] The sex hormones are used to convert stem cells into osteoblasts in the body. Additionally, these sex hormones inhibit osteoclast activity thus decreasing bone density. [55] In terms of repair, the lack of the sex hormones decreases the rate of remodeling of bone tissue. However, these damages begin in the cancellous tissue, then lastly affecting the compact bone tissue. [34] Because the compact bone is targeted last in the series, evidence of bone loss is often hard to detect at early stages. It is not until the compact bone, the structural-loading bearing tissue, degenerates that people begin to have issues with stability.

Secondary causes of bone loss involve actions that can be prevented and do not occur naturally due to low sex hormone levels. Two common causes of secondary bone loss attribute to lack of exercise and vitamins. According to Wolff's Law stating that bone will remodel depending on the loads it experiences; a lack of exercise does not promote densification of bone. [48-49, 54] For healthy, active people, increased loading or continuously loading of the bones promotes growth and densification. Unfortunately, the opposite occurs for those whom are not physically active. The bone adapts to the lack of loading and does not signal the same rate of bone repair and densification. Secondly, the lack of essential vitamins suffocates the osteoblasts restricting the development of bone cells. Vitamin D is needed to efficiently absorb calcium and maintain normal blood levels of calcium and phosphates for biomineralization. [56] Coupled with vitamin D is calcium, calcium is used in the biomineralization process to create hydroxyapatite. The lack of essential vitamins and exercise weaken bones and accelerate the rate of bone loss to a state of osteoporosis.

2.3.2.2 Treatment

The difficult aspect of osteoporosis is early detection as the person affected has no signs unless a bone fracture occurs. Bone mineral density measurements are taken through dual-energy

x-ray absorptiometry. [54, 57] These can be conducted through annual examinations with bone density scans as well. Other experiments on relating the strength of bone with aging showed that every decade the strength of long bones decreases by 3-5%. [58-59] Through routine examinations, early stage of osteoporosis can be detected to start medication to promote bone growth. An anabolic drug known as parathyroid hormone can be taken to reverse the degradation of bone cells and promote bone growth. [31, 60] The drug helps regulate hormone levels which at uncontrolled levels initiate the removal of bone cells but hinder the production of new bone cells. Hormone balancing drugs have shown to reduce the chance of fracture by 40%. [60] Additionally, another drug with positive results in combating osteoporosis is bisphosphonates. These simple molecules contain the starting ingredients for bone growth. [61-62] At the same time, bisphosphonates hinder the metabolic pathways of osteoclasts' resorption of bone cells. [60] While blocking osteoclasts, the bisphosphonates bind to the surface of bone to be mineralized onto bone to thicken the cortical bone section. The downside of bisphosphonates is the efficiency of absorption in the human body. Current orally administered bisphosphonates have a bioavailability of less than 1%. [60, 62] To overcome the issue of poor absorption, the dosages are increased for patient, which can lead to gastrointestinal problems, or the drug is administered intravenously. With all that in mind, the mechanism of these drugs in hindering the osteoclasts' resorption have shown signs of increasing bone growth for those in late stages of osteoporosis.

However, if caught early enough, the rate of bone loss and thinning can be hindered through diet and exercise without the need of hormonal drugs. As stated before, supplementation can prove to be beneficial especially with calcium and vitamin D. [56, 63] The two vitamins need to be taken in unison to promote bone growth, but overdosing on the supplements can cause kidney stones. Therefore, with advanced stages of osteoporosis, supplementation alone will not be enough to prevent bone fracture without side effects. Exercise can strengthen the surrounding muscle to better protect the weakened bone. Although strengthening muscle does not alter bone resorption mechanism, it decreases the chance of fracture through falls or impact. [64] Additionally, load-bearing exercises promote an osteogenic stimulus [65-66] Cyclic and heavy loading forces the bone cells to remodel in order to adapt to loads greater than bodyweight. A sedentary lifestyle does not activate the same stimulus to remodel bones and strengthen them. [66] In its early stages, the rate of bone loss can be slowed down without drugs and through supplementation and exercises.

2.4 Materials for Replacement

A growing field for improving the life of those inflicted with bone diseases is for total bone replacements. These replacements are common for older patients when fracture occurs or the degree of osteoporosis and osteoarthritis reaches severe levels. Common bones for replacements are at the joints, for example the hip and knee. Figure (9) below displays x-rays of both hip and

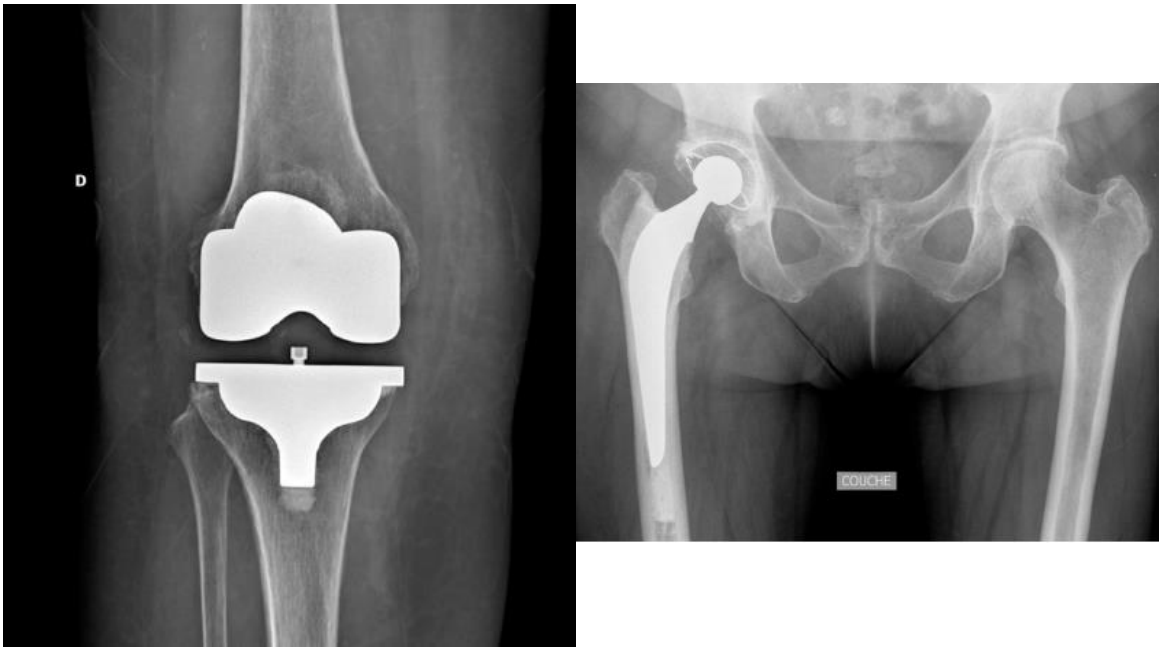

Figure 9: Left: total knee replacement with titanium. Right: total hip replacement with a polyethylene-ceramic ball and socket joint [11]

knee replacements. Important to note is the design of the bone replacement. The cartilage at the joint is removed and the material fully stabilizes lateral movement. [11] With this in mind, the materials for bone replacement have to be wear resistant to prevent infection from broken pieces and ions, have a modulus in range with cortical bone, and have high fatigue strength. Common materials that fit these criteria are metal alloys, high molecular weight polyethylene, and ceramics. Ceramics have seen potential in hip replacement at the socket because of their high wear resistance, but are troublesome on account of their low fatigue strength. Additionally, one ceramic in particular, hydroxyapatite, has been added into composites to promote bone growth and improve osteointegration.

2.4.1.1 Metals

For metals, groups have been exploring the replication of both cortical and spongy bone. An interesting classification of metals has been the cellular metals. This subgroup fabricates metals with a porous network in hopes to incorporate a vascular network. Cellular metals have promise

with their mechanical properties being able to be tuned to mimic ranges of cortical or cancellous bone. Typically, cellular metals aim to have a young's modulus in range with cancellous bone instead of cortical bone. [67] The mechanism osteointegration explains the reasoning behind cancellous bone structure as a target rather than cortical bone. The overall objective of cancellous bone is to provide a matrix for cells to grow into then eventually dissolve classifying the material as biodegradable metal bone replacement. Target goals for this cellular matrix are to incorporate a microporous structure, strength within range of cancellous bone, and little to no metal corrosion. Pure metals such as iron have been studied due to their high strength but lack the ability to control porosity. [67] Therefore, alloys are fabricated to allow control in porosity at the risk of increased corrosion of metal ion leakage into the blood stream. However, a phosphorus-iron alloy have been created showing promise in porosity control, strength, and low corrosion. [67]

Another class of metal implants avoids biodegradation. Porous metals used for structural support and osteointegration have been fabricated. With traditional methods revolving around screws and cements, bone ingrowth can improve the longevity and strength of the implant. Porosity is a significant factor due to the ability to promote bone ingrowth. Two types of porous networks can be obtained, closed-cell and open-cell. Closed-cell pores are a result of random pores fabrication through the introduction of gassing agents in liquid metal often leading to closed pores. [68] Open-cell pores incorporate an interconnected network of open pores developed through sintering and space holder methods. These manufacturing methods permit control over the porosity, pore size, creation of a gradient throughout the bulk. An example of the space holder method can be seen in Figure (10) as a sacrificial material is removed in a metal matrix to create the pores. An SEM image in Figure (11) shows the microstructure consisting of uniform pores. Additionally, open pores' benefits over closed pores involve the ability to remove corroded material and increased osteointegration. [68] Currently in the biomedical, closed-cell porous metals are utilized for dental replacement because of the lesser need for the strength properties and bone ingrowth. Open-cell porous metal see usage in bone replacements; however, in both cases, the increase in porosity decreases the fatigue strength, tensile strength, and increases corrosion for metals. [9] For metals a term known as bone-shielding is used to describe to mismatch in modulus between the implanted material and bone. With bone's bulk modulus ranging from 10-30 GPa and metals having significantly higher bulk modulus such as Titanium at 110 GPa or cobalt-chromium

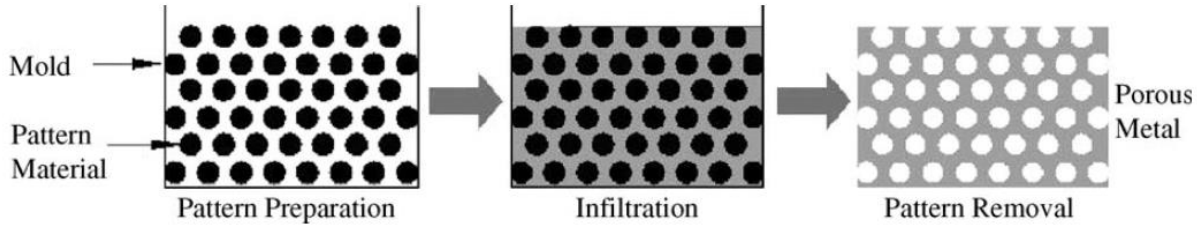

Figure 10: Schematic representation of the three-step replication process. [9]

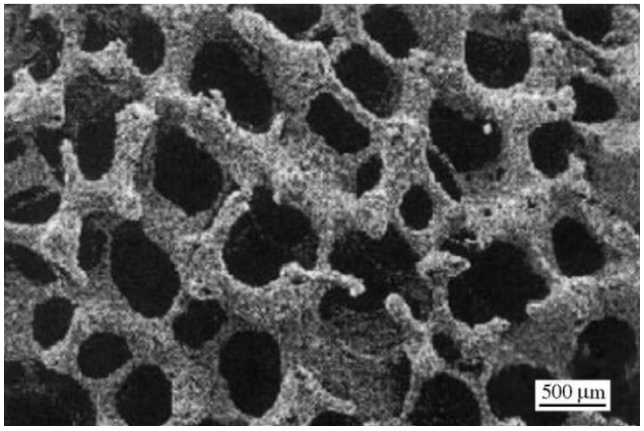

Figure 11: SEM micrograph of porous titanium foam produced by sintering of powders onto a temporary polyurethane scaffold [9]

Alloys at 230 GPa, porosity aids in matching the modulus range of bone. Unfortunately, the porosity must be fine-tuned for the metal as the high surface area promotes more corrosion because of high area for reactive sites. Nevertheless, studies have shown that highly networked open pores increase corrosion resistance because of the free flow of ionic species. An entrapment of the ionic species prevents the development of passive corrosion resistant passive layers. [69] Bioactivity is dependent on the network of open pores; however, the volume percent of pores must be fine-tuned to balance out the negative strength and corrosive properties.

As previously mentioned, titanium is a metal studied for bone replacement as it exhibits high corrosion resistance and mechanical properties in the upper range of bone. The downside of titanium is the lack of bioactivity; in order to counter this, hydroxyapatite is introduced to develop a biocomposite. Hydroxyapatite is a ceramic proven to promote osseoconduction with a chemical structure similar to human bone. [1, 19] However, the ceramic does not possess the tensile properties needed to replace bone on its own. Therefore, the two materials are blended together to produce a composite within the modulus range of human bone. Looking further into a popular metal for bone replacement, titanium has been studied because it is biocompatible, optimal strength properties, but lacks bioactivity. To tackle the lack of bioactivity, hydroxyapatite is embedded into a titanium

matrix to promote bone cell growth. Fabrication of the titanium-hydroxyapatite composite has been performed with sparked pulse sintering. Sparked pulse sintering combined with a space method has been proven to develop porous composite of the two materials. [1] The sintering process exhibits control over the pore size by controlling the degree of necking from a bulk titanium powder. Images taken by back-scattered electron microscopy shown in Figure (12) display the work of Zhang et al. With their study, it was shown that up to 30wt% hydroxyapatite can be added titanium through the sparked pulse sintering method, and with increased hydroxyapatite rose an increase in porosity. [1, 70] Increased porosity was beneficial by initiating interconnected pores; thus, the process created an open-cell porous network optimal for bone ingrowth. Coupled with BSEM, the study tested the mechanical properties of the titanium-hydroxyapatite composites. Keep in

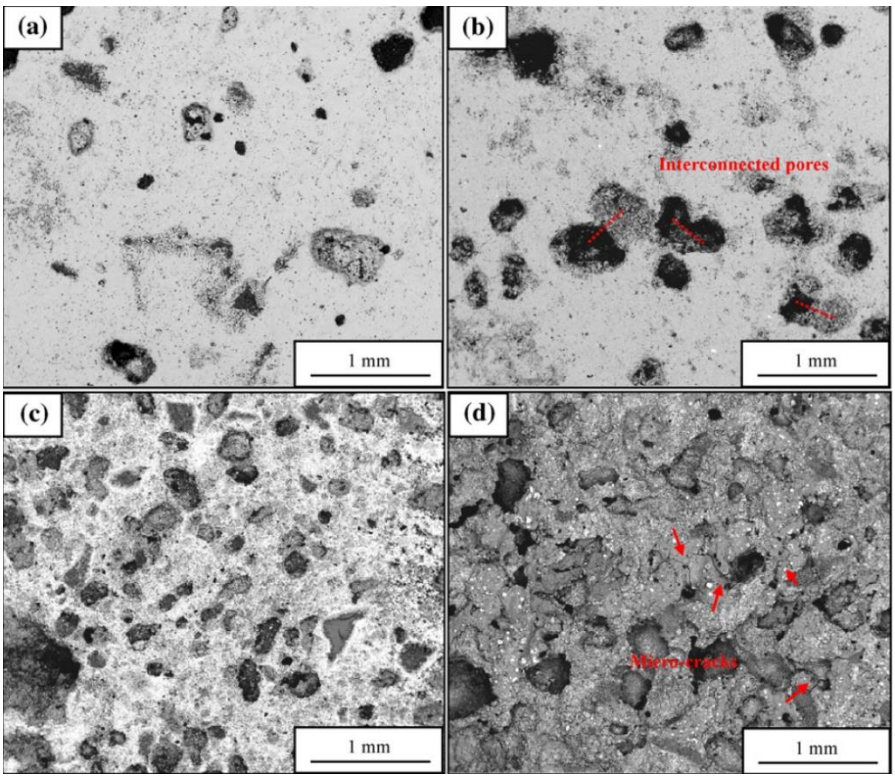

Figure 12: Porous surface of the porous Ti-HA biocomposites prepared by SPS with different contents of HA: (a) 5 wt%, (b) 10 wt%, (c) 20 wt% and (d) 30 wt%. [1-3]

mind, the objective of the composite to achieve a modulus in range with cortical bone at 2-20 GPa. [1] The composites' modulus decreased with increased hydroxyapatite content. At 30wt% hydroxyapatite, the modulus ranged from 8.2 to 15.6 GPa with roughly 60% porosity matching the properties of cortical bone. [1] Coupled with mechanical testing, studies have investigated the corrosion of titanium-hydroxyapatite composites for ion leaching. Unfortunately, the increase in

porosity decreased the corrosion resistance of the composite compared to neat titanium, the titanium-hydroxyapatite interface served to entrap pores creating microcracks in the bulk structure instead of creating open pores for free ion species to flow. [70] Achieving a composite with a modulus in range with cortical illustrates potential in porous titanium based composites for bone replacement.

2.4.1.2 Ceramics

Once again, the target mechanical properties for bioceramics revolve around current studies found in compact and cancellous bone. As CaPs exhibit high levels of bioactivity, their studies are compared to both compact and cancellous bone in multiple modes of stress. However, by being a ceramic, their resistance to crack propagation leaves them unsuitable for replacing bone entirely. Furthermore, to avoid mechanical data failing from crack propagation, mechanical properties in compression or flexion are often tested for CaPs. Hydroxyapatite has recorded compressive elastic modulus of near 50 GPa and a compressive strength of 174MPa. [71] These values are within range of cortical bone, but higher than cancellous bone. The bioactivity of CaPs makes them an essential component for bone replacements and alone they show promise in mechanical properties.

CaPs are excellent for their bioactivity but due to their lack of resistance to crack propagation, CaPs are used a filler component for composites. The composite matrices consist either of a metal such as titanium or a polymer such as poly(ether ether ketone). For metals, the introduction of CaPs, more specifically hydroxyapatite, HA, changes the microstructure to introduce porosity while lowering the modulus to prevent bone-shielding. For polymers, HA improves the strength of the composite to reach modulus values similar to cortical or cancellous bone. However, for both metal and polymer composites, the HA does not bond with the matrix making for increased voids leading to a lower fracture toughness that is compensated by the ductile polymer or metal matrix. Compared to HA alone at the same porosities, the mechanical properties of the composites are greater.

The ceramic class of calcium phosphates, CaP, or also known as bioceramics proves to be an ideal material for bone replacements. For osteointegration, CaPs have properties tuned to promote bone growth. Hydroxyapatite and β-tricalcium phosphate are studied extensively due to their resemblance and abundance in human bone. With a structure and composition similar to human bone and the ability to induce bone growth, the human bone naturally adheres to the

material instilling bioactivity. [72] Additionally, CaPs degrade or are bioabsorbed at a controlled, slow rate. The rate of degradation can be controlled by varying the composition of biphasic calcium phosphate (BCP) which is the ratio of hydroxyapatite to β-tricalcium phosphate. [72] Depending on the function of the implanted material, a fast degradation rate can be used to create a replacement to be absorbed by the body and act as a sacrificial scaffold, or a slow degradation rate can be used for a replacement composite to provide structural support for the bone.

2.4.1.3 Polymers

Compared to the other classes of materials, polymers are often the most ductile yet lowest in strength. The processing parameters and ability to develop composites give polymers potential in mimicking the properties needed to replace bone. These composites can contain oriented fibers to replicate the structure of cortical or have particles of hydroxyapatite to increase the overall strength and promote bone growth. Due to the low modulus of polymers, the maximum amount of filler content is aimed for to best strength and osteointegration. However, the filler content is limited by the processing and interface strength between the polymer and hydroxyapatite. Typical polymers used to produce these composites are HDPE and PEEK.

Currently, high density polyethylene, HDPE, is utilized to create the cup joint for polymer-metal bone replacements. HDPE's high strength to weight, bio-inertness, and wear resistance make it ideal for bone replacement. [13] With a young's modulus of 0.8 to 1 GPa, HDPE is a little low in the modulus range seen for bone. [13] The introduction of hydroxyapatite particles aid in increasing the young's modulus to be in range. Studies have shown that with increasing hydroxyapatite content there is a linear increase in young's modulus with an exponential loss in elongation at break. [13] Hydroxyapatite addition to HDPE shows promise but the content of HA is limited by the melt extrusion process used in the production of the HDPE/HA composites. With increasing HA content, the viscosity increases and the dispersion of HA within the composite becomes non-uniform. Due to the solubility limitations, HDPE is limited to these melt processing conditions. 50wt% or 25vol% HA has been blended into a HDPE matrix; however, at this composition, the modulus of the composite registered at 2.5 GPa with the lower bound of bone being 3 GPa. [12-13] The SEM image shown in Figure 10 displays the integration of an HA particle in HDPE. [73] Extrusion molding was performed to produce the composite. The image shows that at the interface of the HDPE and HA there is void space which can contribute to a lessening of the yield strength of the composite. Additionally, the amount of energy absorbed through impacts decreases with

increasing HA content. For flat bones, the lessening of impact resistance isn't ideal, but for long bones the impact resistance isn't as important as long as the structure and modulus can be replicated. The voids act as stress concentrations and paths for crack propagation.[74] These factors contribute to the lowering of the toughness of the composite to cyclic loading and impact. [74] In order to improve the mechanical properties further, the molecular weight of HDPE can be increased. UHWPE has been studies for bone replacements but the processing limitations are greater due to the higher molecular weight. Instead blends of UHWPE and HDPE have been studied to observe any chances in mechanical properties. Shown in Figure (13) and (14), the impact strength of the blends dramatically decreased with the introduction of HA. The modulus of the blend did not surpass the HDPE. However, the blend showcased the ability to have more content of HA. Therefore, the blend can achieve higher values of modulus while improving the ability for bone cell growth. With the increase in modulus, the blend showed a severe drop in impact strength

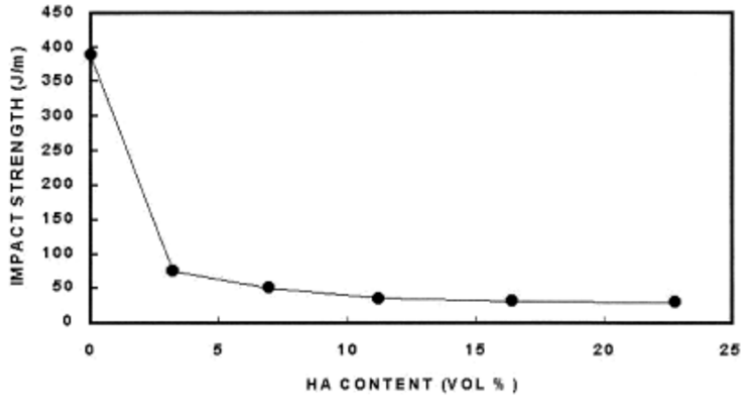

Figure 13: Impact Strength vs. HA Content of 50:50 HDPE:UHMWPE Blends [13]

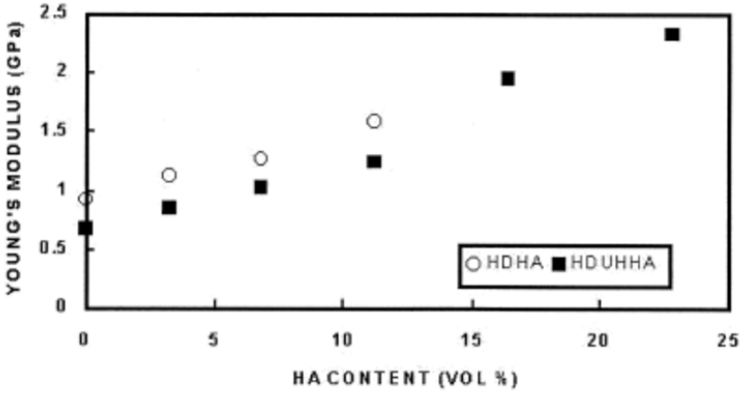

Figure 14: Young's modulus of HDPE and HDPE/UHMWPE blends vs. HA content [13]

with the addition of HA. The voids created at the interface of the HA and HDPE:UHMWPE blend lessen the toughness of the composite.

However, the same image shows great embedment of the HA particle in the HDPE. Through bone cell growth studies, the composite has proven to promote bone growth and adhesion of cellular structures to the matrix of HDPE. [73] The assumption is, through the integration of bone cells through the matrix of the HDPE as the hydroxyapatite would be consumed and replaced by bone cells, after the bone growth the mechanical properties of the composite would increase. Compared to HDPE on its own, the implant would have an interconnected network of cells to anchor into place. This would help reduce the effects of bone shielding along with the lessening of toughness as the bulk of the material is integrated and filled from voids. Additionally, the modulus of the composite would match closer to that of bone with bone cells integrated within. [73] Unfortunately mechanical testing of HDPE/HA after bone cell growth are estimations. Similar to the mechanical testing on bone itself, the conditions of the tissue would play a large factor in the mechanical properties as the freshness of the tissue and environment would dictate the mechanical properties.

Another polymer with greater mechanical properties than HDPE has been studied as a potential replacement for bone. Poly(ether ether ketone), PEEK, has a young's modulus of 3.5 GPa and tensile yield strength of 97 MPa. [75] These values on their own are in the lower bound of bone to prevent bone shielding in replacements.

Similar to HDPE, PEEK requires melt extrusion or injection molding processes to create composites with hydroxyapatite due to its insoluble with regular organic solvents. [12, 22] Known solvents to dissolve PEEK are highly concentrated acids such as sulphuric acid. [76-77] Solution casting provides multiple advantages for the biomedical field such as creating custom fit parts. These parts can be casted through sacrificial or reverse cast molds seen in metals casting. Additionally, injection molding's high pressure and temperature settings limits the additives due to the thermal degradation. Because of this, PEEK composites have been dominated by ceramic-PEEK composites. Examples of these composites are carbon-fiber reinforced PEEK developed to increase mechanical strength. [78] Oriented long-fibers show promise in mimicking the anisotropic structure of cortical bone, but the additive aids in strength properties not in biocompatibility. However, another reason solution casting has been avoided for PEEK is the lack of solubility in PEEK. Highly concentrated sulfuric acid chemically alters the PEEK creating what is known as

Sulphonated-PEEK (S-PEEK). [75, 77] The chemical altering affects multiple key properties of PEEK such as a decrease in young's modulus, elongation at break, and thermal stability with a first onset at 390 °C [77].

Nevertheless, studies have been done to develop PEEK/HA composites for bone replacements through melt processing. Melt processing has created PEEK/HA composites with a greater content of HA than compared to HDPE. Shown in the Figure (15) below, a PEEK matrix has the capability to incorporate up to 40 vol% of HA with higher modulus values. The largest increase in modulus can be seen at 40 vol% of HA and even after cyclic loading, the PEEK

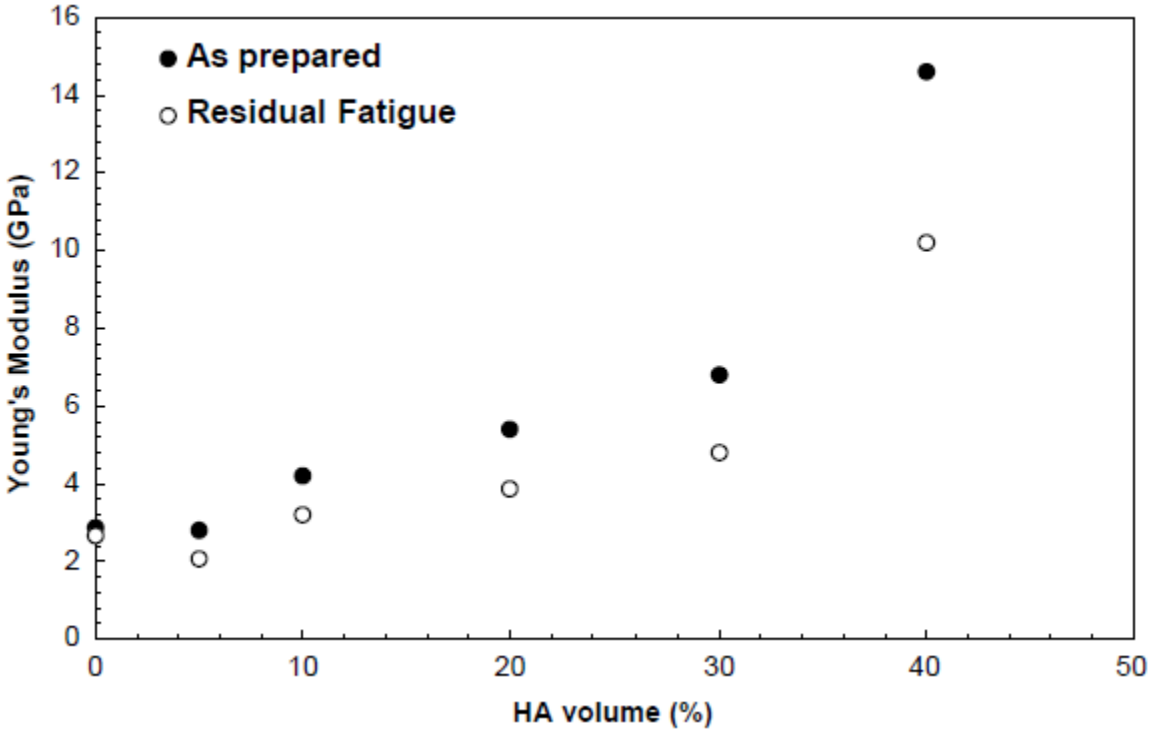

Figure 15: Young's modulus of PEEK/HA composites before and after cyclic loading[12]

composite's modulus is in the modulus range of bone. Although the high-volume content of HA increased the modulus of the composite, the porosity of the composite increased to 60% versus 5% for neat PEEK. [12] The increase in porosity can be contributed to the interface voids of the HA and PEEK. Porosity is beneficial in replicating the structure cancellous bone, but decreases the yield strength and toughness of the composite. Even with a decrease in yield strength the PEEK/HA composite's yield strength was in range of bone at 90 MPa. [12] The decrease in yield strength can be correlated to the poor bonding between the HA and PEEK. Seen in the Figure (16) below, SEM

imaging of a fractured surface of PEEK/HA shows fracture due to debonding of the HA and PEEK. [12] The HA that once filled the spherical voids are sites for crack propagation.

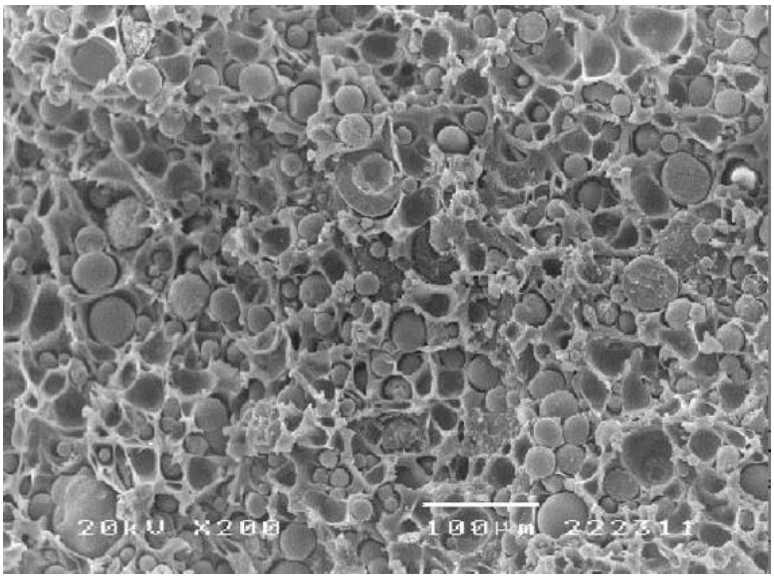

Figure 16: SEM image of fractured surface of 40 vol% HA in PEEK from injection molding [12]

Regardless, the volume percentage of hydroxyapatite improves the osteointegration of the composite. Larger amounts of HA as proven to increase the rate of bone growth as well. [21-22] Studies conducted on pig bone showed mature bone growth filling in the voids of PEEK/HA composites within 6 weeks. [12, 21] At the same time, the PEEK/HA composites *in vitro* showed no sign of toxicity to the body which can be seen with metal implants. [22] One concern not taken into account for both HDPE and PEEK is the removal of fracture polymer that could be possible in the early stages of bone growth due to cyclic loading or impacts. Small pieces of polymer floating in the body may or may not cause a biological response similar to how metal ions released into the blood stream cause inflammation. Regardless, the filling of voids through bone cell growth is beneficial towards the mechanical properties of the bone replacement. The growth of collagen fibers is evident but not the production of marrow. Additionally, the bone growth helps replicate the dense structure of cortical bone, but not for cancellous bone. Studies still need to be conducted to determine if the voids are filled by replacing the existing HA or through the pathway of growth in bone cells. Combined with mechanical properties in range with bone, the ability to host bone cell growth makes PEEK/HA composites capable of replicate bone that can not only replace existing but promote bone growth for full integration to the body.

3 PEEK/CNC Nanocomposite

3.1 Materials and Methods

3.1.1 Materials

Poly(ether-ether ketone) powder was acquired from Victrex 150PF with a particle size of 50 microns. 4-chlorophenol and hydroxyapatite were obtained from Sigma-Aldrich. Ethanol was purchased from Fisher Scientific. Dried cellulose nanocrystals (CNCs) were obtained from Forest Products Labs. All materials were used without any modifications.

3.1.2 Sample Preparation

3.1.2.1 Dissolution of PEEK in Chlorophenol

For samples containing CNCs, the desired amount of CNCs was added to melted chlorophenol at 90 °C and stirred for an hour. CNC compositions consisted of 0, 5, 10, and 20 weight percent. The CNC solution was sonicated until a dispersion of CNCs was created before adding PEEK to create at 15w/v% solution of PEEK to chlorophenol. [76] The final solution was heated at 150 °C for 6 hours. After 6 hours, the solution was sonicated for 10 minutes then 20mL of the solution was poured into a 50mL beaker to let sit at ambient conditions for 24 hours.

3.1.2.2 Solvent Exchange Chlorophenol into Ethanol

Once the casted samples gelled, a solvent exchange with ethanol was performed for the removal of chlorophenol. Ethanol was poured onto the sample directly. A color change from brown to grey was observed indicating the removal of chlorophenol. Additionally, a change in the color for the ethanol solution was monitored as the chlorophenol developed a yellow-orange tint. After letting sit for 5-10 minutes, the ethanol supernatant was discarded and additional ethanol was added. The process was repeated until the color of the sample was grey and the stiffness was sufficient for handling. Then the sample was transferred into a 200mL bath of ethanol with the ethanol removed and replaced three times within a 24-hour period. Additionally, to evaluate solvent systems, samples in the ethanol bath were solvent exchanged with water using the same washing procedure.

3.1.2.3 Drying of the PEEK/CNC Composite

Samples were taken out of the ethanol bath and left to dry at ambient conditions for 24-hours. Additional samples were dried in the vacuum at 50 °C and 120 °C for 24 hours. During

drying at atmospheric pressure shrinkage of the PEEK casts can be seen. For later scanning electron microscopy, a set of films were freeze-dried at .07 barr after being taken out of the ethanol bath bypassing drying at ambient conditions.

3.1.3 Characterization of PEEK/CNC Composite

3.1.3.1 Thermogravimetric Analysis

Thermogravimetric analysis was performed with a TA Q500. The temperature ranged from 25 °C to 1000 °C with a heating rate of 10 °C/min. The tests were carried under nitrogen with a flow rate of 40mL/min. All results were analyzed using the Universal Analysis software.

3.1.3.2 Differential Scanning Calorimetry

Differential scanning calorimetry was performed with a TA Q20. The heat and cooling cycles ranged from 50 °C to 400 °C at a heating rates of 10 °C/min and a cooling rate of 10 °C/min. The tested were carried under nitrogen with a flow rate of 40mL/min. All results were analyzed using the Universal Analysis software. Chlorophenol and PEEK solution experiments were conducted with TZERO hemetic pans and lids.

3.1.3.3 Scanning Electron Microscopy

Scanning electron microscopy was conducted at the Nanoscale Characterization and Fabrication Laboratory using the LEO (Zeiss) 1550 field-emission SEM. Samples were coated with 5nm of High-Resolution Iridium and painted with conductive graphite paint before imaging. Surface and fractured images were taken with the fractured samples being broken under liquid nitrogen.

3.1.3.4 Mechanical Testing

During sample preparation, solutions were casted into dogbone molds at ASTM 638D dimensions. Compression samples were casted into 50mL beakers with a height:diameter ratio of 3:1. All compression and tensile tests were performed on an Instron. The load cell for compression tests was 50 kN with a strain rate of 1mm/min. Tension tests were conducted with a load cell of 500N with a strain rate of 0.5mm/min.

3.2 Results and Discussion

3.2.1 SEM Imaging

Scanning electron microscopy (SEM) revealed varying porous structures achieved depending on the drying method. Samples freeze-dried displayed a higher porosity than those left to dry at ambient conditions due to the lack of shrinkage seen when allowing samples to dry at ambient conditions. Figure (17) displays a comparison in structure of freeze-dried and ambient-dried PEEK at the surface and fracture faces. The surfaces' pore sizes are similar being in the mesoporous range for both the freeze-dried and ambient-dried samples. However, the fractured faces display a difference in average pore size when comparing the two drying methods. During freeze-drying, the quick removal of the solvent through sublimation left behind a nanoporous structure seen in Figure (17c). The pore size range can be seen in Figure (18) with pores ranging from 50-200 nm in size. The slow removal of the solvent from ambient-drying allowed for the collapse of the porous structure leaving a dense structure with little evidence of pores. The

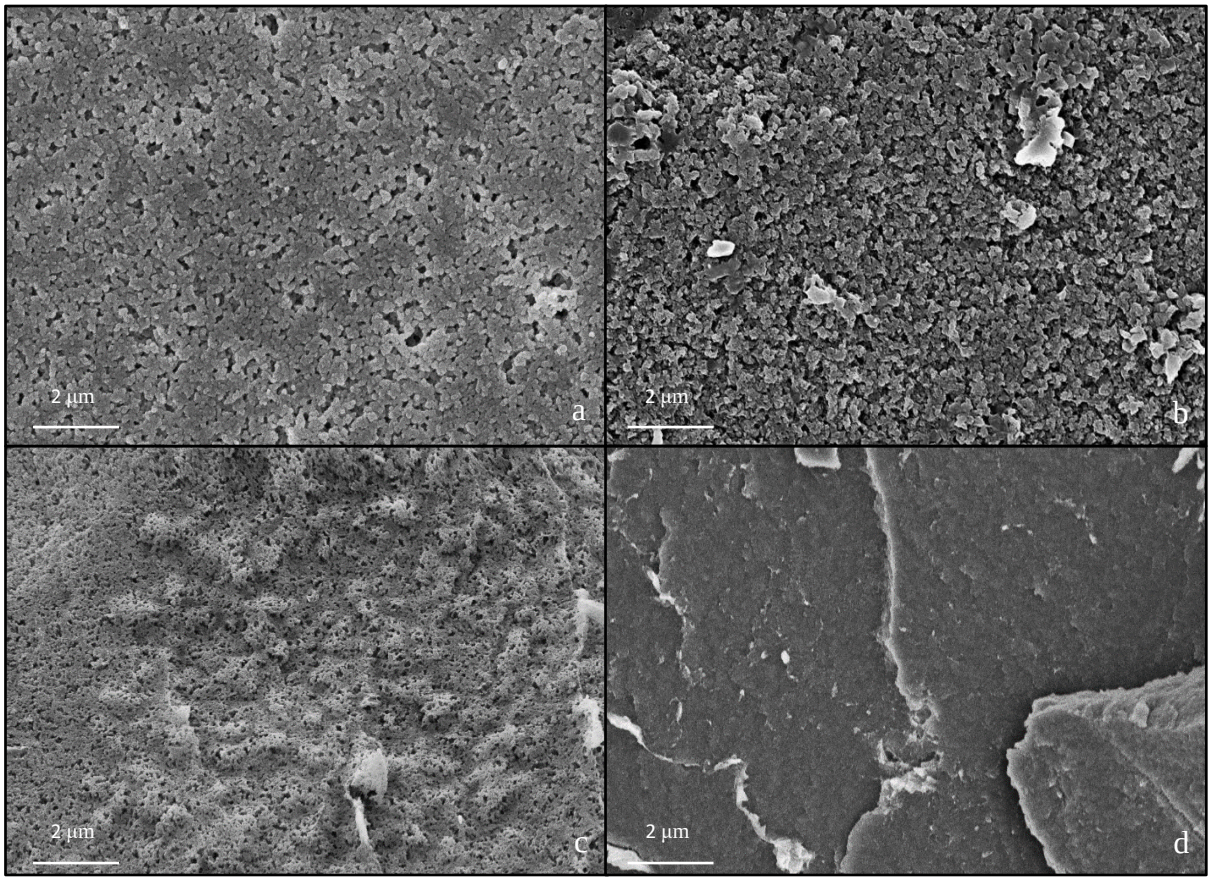

Figure 17: SEM images of PEEK dried from ethanol a) surface freeze-dried b) surface ambient-dried c) fractured freeze-dried d) fractured ambient-dried

difference in porosity from processing can lead to a gradient in structure similar to the cancellous and cortical bone interface. However, the average pore size from freeze-drying is too small for housing cellular growth, but is in range for mineral deposits of calcium.

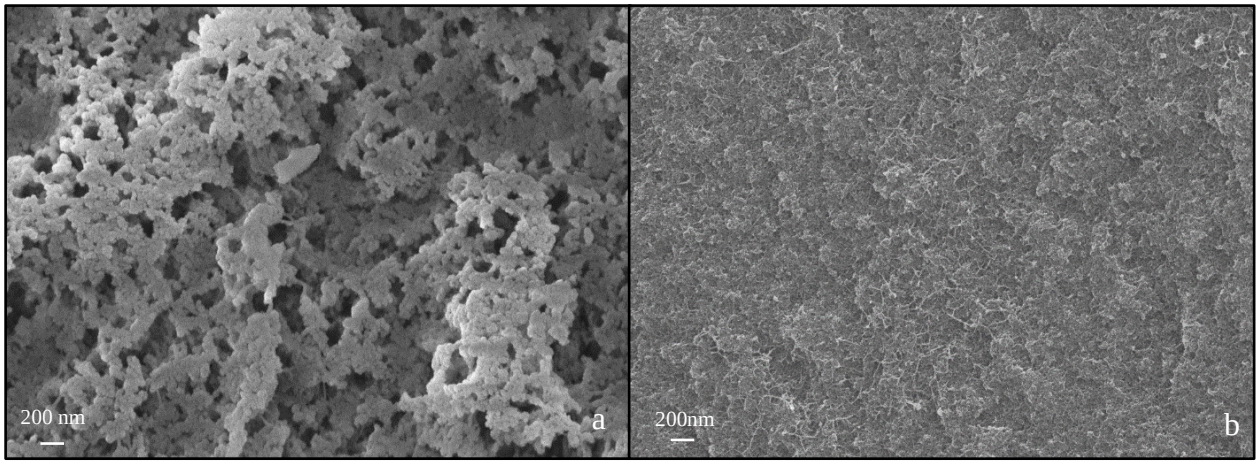

Figure 18: SEM image of PEEK dried from ethanol a) fractured freeze-dried b) fractured ambient-dried

In order to look at the variance in structure from different solvents being utilized, water was used as an alternate solvent in the solvent exchange process. After an ethanol solvent exchange, samples were washed in DI water baths to solvent exchange from ethanol to water. Figure (19) displays surface images of PEEK dried at ambient conditions from ethanol and water baths. Both solvents produced a granular surface structure. It is speculated that the solvent's role in the structure may not be significant, however, the drying method dictates the structure because of the effect capillary forces. The slow evaporation from the liquid state generates the capillary pressure to compress the PEEK inducing the shrinkage. A schematic seen in Figure (20) illustrates the size change during drying. As the liquid-solid interface is energetically favorable compared to a liquid-gas interface, a meniscus of the solvent within the pores is developed during drying. [79] The meniscus extends the solvent's contact area with the PEEK creating a tensile force against the

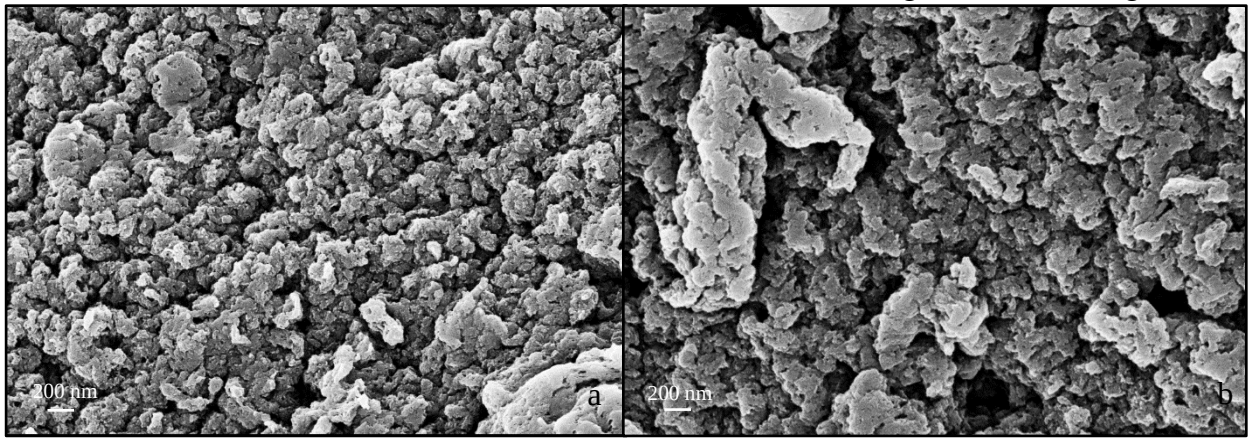

Figure 19: PEEK dried from a) water b) ethanol

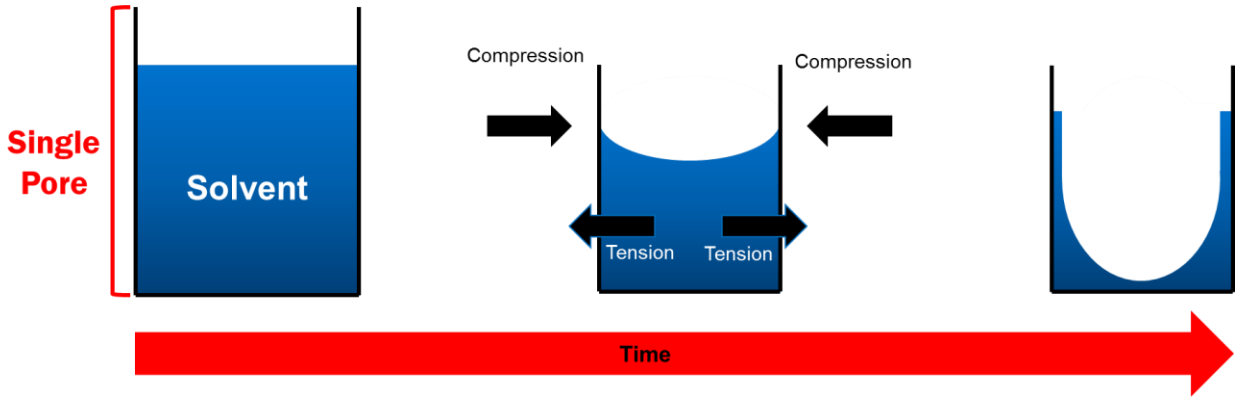

Figure 20: Schematic of pore shrinkage as a result of capillary pressure

PEEK. In order to balance forces, a compressive force from the PEEK acts against the solvent. This compressive force drives the shrinkage in the PEEK. Interesting to note is the compressive and tensile forces resulting from the capillary pressure can leave residual stresses within the PEEK matrix. These residual stresses can lead to stress concentrations and lower of strength. Scaling up to a network of pores, the capillary pressure and shrinkage can result in a mixture of open and closed pores in the PEEK. As the PEEK begins to shrink, the pores within the bulk do not have contact with air leaving solvent entrapped. At this point of the drying, the closed pores rely on diffusion through the PEEK in order to be removed. With solvent entrapped within the PEEK matrix, it can be inferred that the remaining solvent acts as a plasticizer, thus altering the glass transition temperature. In addition, the compacting of the structure can be contributed to secondary crystallization in the amorphous phase. Figure (21) displays the progression of crystal formation throughout the solvent exchange and drying process. During the removal of chlorophenol, a saturated solution of PEEK is left behind giving rise to crystal formation. The crystals formed in the amorphous phase are distanced by the ethanol. Once the removal of ethanol begins, the

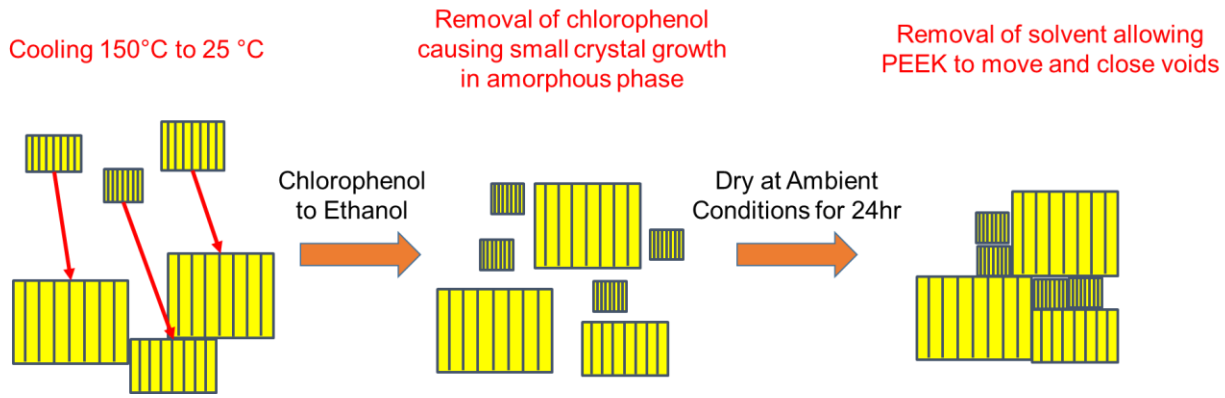

Figure 21: Schematic of PEEK shrinkage as a result of secondary crystal formation

secondary crystals move towards the primary crystals leading to the PEEK shrinking and closing existing pores.

Additives were added to the PEEK to create a nanocomposite. CNCs were added in solution and sonicated for dispersion. However, with the scale of the SEM, visual representation of CNCs were not achieved. The evidence of CNCS were confirmed later with thermogravimetric analysis. Another additive, hydroxyapatite (HA) was added in solution and sonicated similar to the CNCs. SEM imaging confirms the dispersion and addition of the HA spheres into the matrix of the PEEK. Figure (22) highlights the structure and embedment of the HA spheres within the PEEK matrix. The red circles outline the HA particles in the size range of 200 nm. Coupled with the information from Sigma-Aldrich, these images confirmed the integration of HA within the PEEK. Both the freeze-dried and ambient-dried samples displayed the presence of HA. Bone growth studies can be performed on the porous PEEK/HA composite to observe if the pore sizes are the right size. At 30wt% HA, the volume percentage of HA is near 15%. The low volume percentage may explain the low concentration of HA in the SEM images. With the goal of promoting bone cell growth, a higher concentration of HA would in theory provide optimal conditions for cell differentation. Also, with HA being consumed during bone cell growth, a perculating network of HA particles can be simulate the same structure as a porous network.

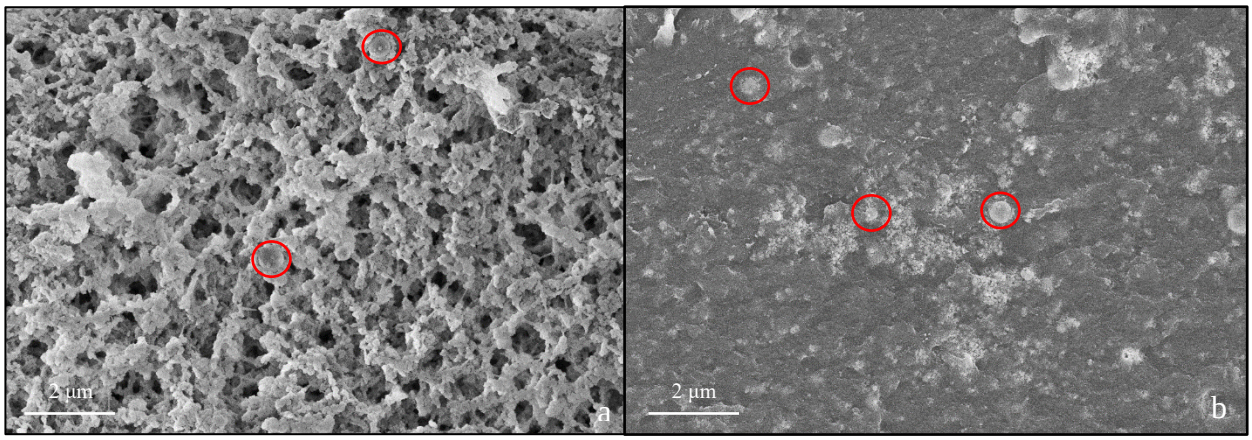

Figure 22: SEM image of 30wt% nHA in PEEK dried from ethanol a) fractured freeze-dried b) fractured ambient-dried

3.2.2 DSC Data

Differential scanning calorimetry experiments were conducted to observe any thermal changes as a result of the solution casting process. As a control, the PEEK powder was tested as received. Seen in Figure (23), the PEEK powder's melting and crystallization temperatures were measured at 344 °C and 300 °C. Using the universal analysis software, a glass transition step was

recorded at 148 °C on the second heat curve for both the PEEK powder and casted PEEK after ambient drying. Looking at the first heat for the curves in Figure (23), the ambient-dried PEEK displayed a broad endothermic peak not exhibited in the PEEK powder. Because the broad peak is near the T_g of PEEK, it is thought that the broad peak is a result of leftover solvent in the system acting as a plasticizer. Additionally, the crystallization temperature decreases from 300 °C to 290 °C from the PEEK powder to the casted PEEK. Plasticizer content increases the mobility of chains in the amorphous phase leading to less required energy to induce crystallization. Additionally,

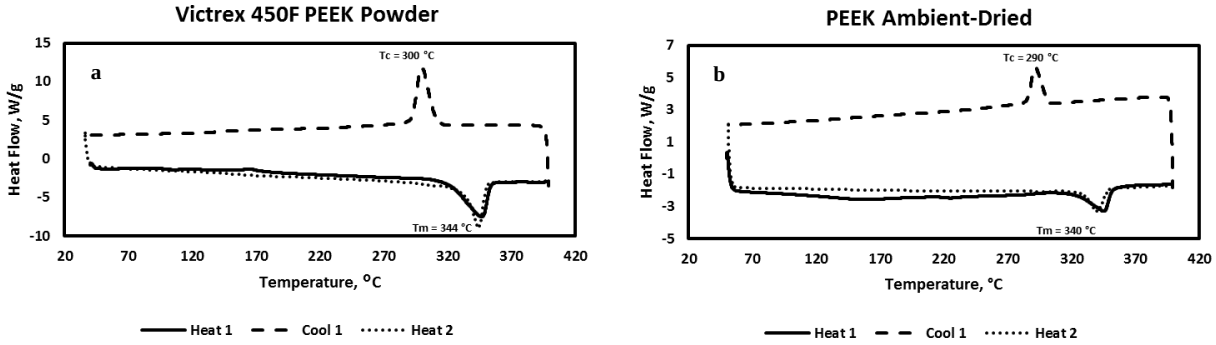

Figure 23: Exo-up DSC curves of a) PEEK powder as received from Victrex and b) PEEK after ambient-drying for 24 hours

plasticizers can act as impurities allowing for less energy needed to start crystal nucleation. The crystallization temperature difference is coupled with a difference in the heat of enthalpy of the two PEEK samples. For the powder, the crystallization enthalpy taken from the integration of the crystal peak was recorded at 60 J/g, while the crystallization enthalpy for the casted and ambient-dried PEEK was recorded at 35 J/g. The decrease in required energy for crystallization can help explain the idea of secondary crystal formation from casting and solvent exchange process. In an attempt to develop a composite free of remaining solvent, PEEK from both ethanol and water baths were vacuum dried at 120 °C for 24 hours after the initial 24 hours of drying at ambient conditions. 120 °C was chosen to boil off the remaining solvent in the system as well as increase the rate of diffusion. Figure (24) shows how drying at 120 °C lessened the intensity of the broad peak that was previously seen in the ambient-dried PEEK. PEEK dried from a water bath displayed a near overlap in the first and second heating curves. PEEK dried from an ethanol bath showed a small endothermic broad peak. Although dried at an elevated temperature, remaining ethanol and

chlorophenol solution or PEEK and chlorophenol solution could be present. The combination of water being less miscible with PEEK and chlorophenol than ethanol as well as having the PEEK samples washed an additional three times can explain the overlap in the first and second heat curves. Looking at the crystallization peaks, the crystallization temperatures increased compared to the powder and ambient-dried samples. With crystallization enthalpies at 66 J/g for ethanol and 57 J/g for water, there is an increase in energy required when compared to the ambient-dried PEEK. At the elevated drying temperature, the secondary crystals formed during the ambient-drying phase can be given enough time and energy to grow in size. The lower plasticizer content can decrease the mobility of chains in the amorphous phase, as well as removing impurities in the system that would require less energy for nucleation.

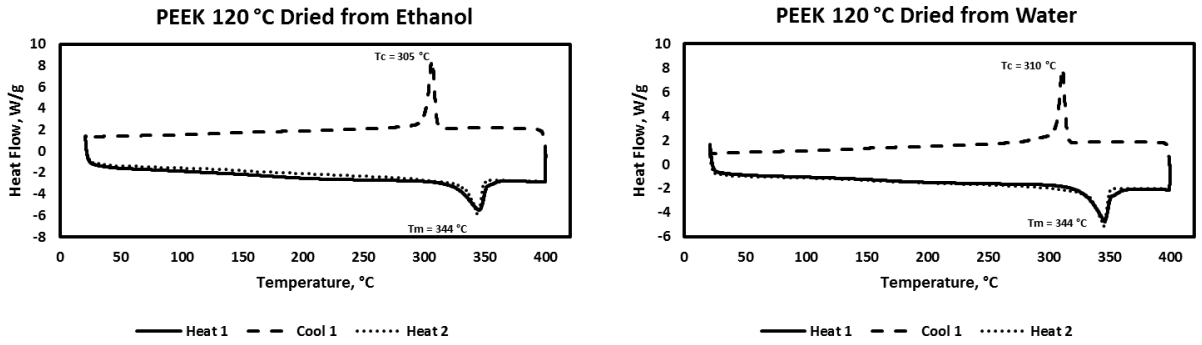

Figure 24: Exo-up DSC curves of PEEK dried at ambient conditions for 24 hours then in a vacuum oven for 24 hours from an ethanol bath and water bath

3.2.3 TGA Data

Thermogravimetric analysis was performed to confirm additive concentration of the CNCs and HA. Additionally, degradation points of the PEEK were compared to those of literature to observe any changes in thermal stability that could have resulted from the solvent casting process. With ambient-drying, the onset of degradation was 670 °C seen in Figure (25). Compared to literature values, the degradation is in range. [80-81]. Besides an initial loss in weight due to ethanol evaporating, "wet" PEEK, or PEEK taken immediately out of the ethanol bath, showed an onset of degradation at 670 °C. Samples heated at 120 °C were tested as well. Unfortunately, with the extended time at an elevated temperature, the thermal stability of the PEEK decreased shown in Figure (25). A constant weight loss occurred until 400 °C with an overall weight loss of 20%. Due to the constant weight loss and plateau at 400 °C, the initial weight loss is thought to be contamination from leftover chemicals within the oven. Although the objective for the increased

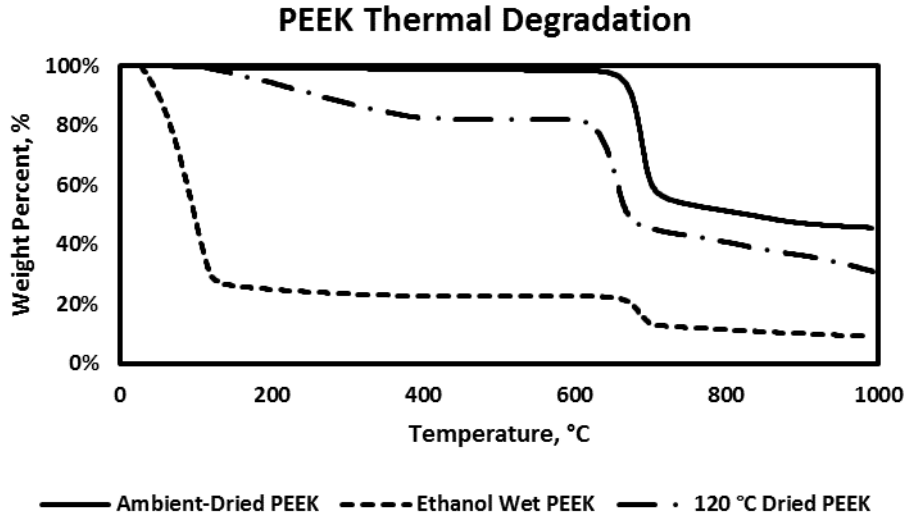

Figure 25: TGA of PEEK at three different drying stages

drying temperature was to promote diffusion of the entrapped solvent out of the PEEK, drying at 120 °C could have allowed for solvents remaining in the oven to diffuse into the PEEK.

For samples containing additives, the TGA showed a successful integration of the CNCs and HA within the PEEK matrix. Shown in Figure (26), the first onset for the 20wt% CNC sample is at 330 °C which is in range of literature values for CNC degradation. [82] The weight loss before 330 °C can be attributed to water evaporating as CNCs are hydrophilic. Similarly, the HA composites showed a small amount of weight loss caused by the dehydration of the HA particles. [83] The additional additives did not interfere with the degradation of PEEK. The weight loss

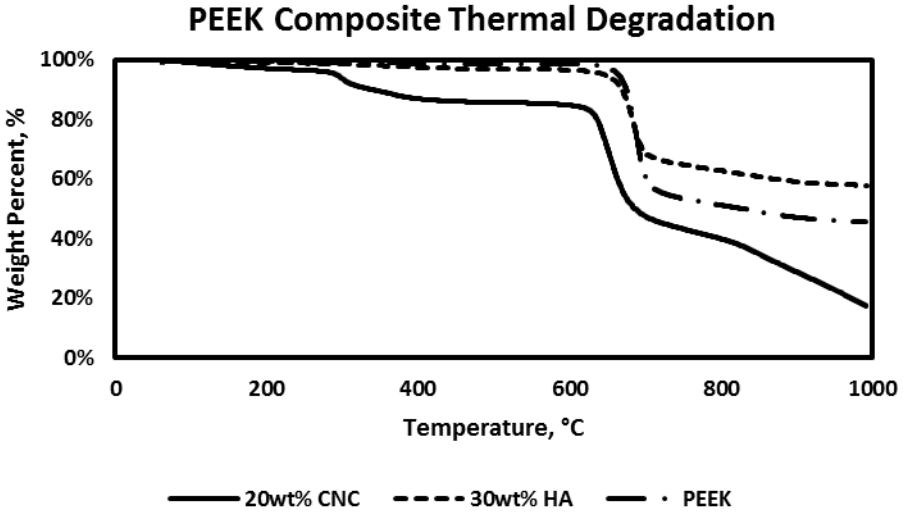

Figure 26: TGA of PEEK composites dried at ambient-conditions

difference between the HA and pure PEEK samples did not match the intended 30wt%. Instead a 15wt% loss can be seen which can be contributed to a lack of proper dispersion of the hydroxyapatite particles from solution casting. For processing, having the CNCs at 150 °C in solution did not destroy the CNCs and provides promise for other low temperature additives that can be added to PEEK if proper dispersion can be achieved.

3.2.4 Tensile Data

Tensile testing was performed to observe the effect of varying CNC content on the mechanical properties of PEEK. Samples tested under tension were dried at ambient conditions. Although previous DSC scans showed evidence of plasticization, the stress vs. strain curved displayed brittle fracture. The lack of ductility can be attributed to the porous and granular structure seen in the SEM images. The pores/voids create stress concentrations leading to fracture at low stresses. Looking at Table (1) and Figure (27), the modulus of the PEEK and the PEEK/CNC composites varied inconsistently. For CNC reinforcement, polymer composites have been seen to have an increase in modulus with increasing CNC content. At 5wt% CNC, the composite shows a decrease in modulus with an increase in elongation at break when compared to pure PEEK. Due to CNCs being hydrophilic, the absorption of water or ethanol in the cellulose can further plasticize the composite. At 10wt% the modulus nearly doubled that of pure PEEK showing the

Table 1: Mechanical data of PEEK/CNC composites in tension

CNC Weight Percent	Young's Modulus, MPa	Elongation at Break, %	Yield Strength, MPa
0	258 ± 19	0.050 ± 0.0	11.9 ± 0.9
5	101 ± 2.4	0.100 ± .02	6.1 ± 0.2
10	442 ± 23	0.023 ± 0.0	8.3 ± 0.7
20	185 ± 11	0.063 ± 0.01	11.2 ± 1

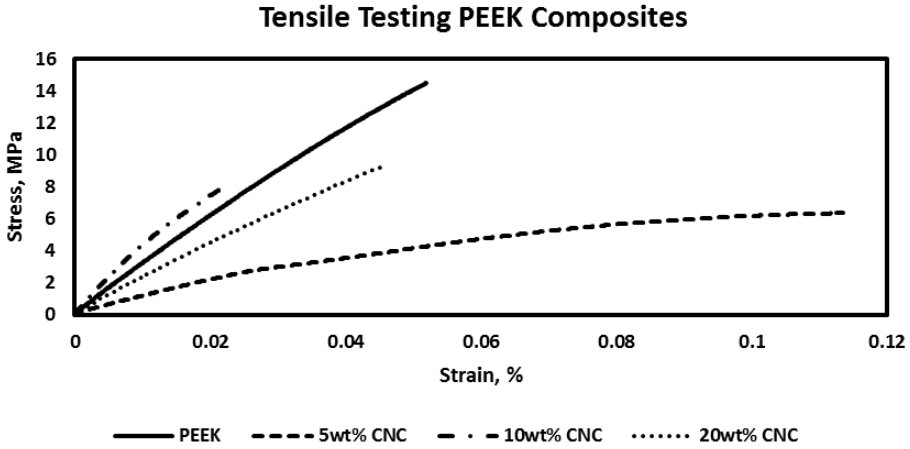

Figure 27: Stress vs. strain plots of PEEK/CNC composites in tension

reinforcement properties of CNCs. The increase in modulus displayed reinforcement yet did not explain correlate with the plasticization from solvent attached to the hydrophilic CNCs. At 20wt% CNC, the modulus was lower than the pure PEEK yet slightly higher than the 5wt% CNC composite. 20wt% CNC could be an upper limit for CNC concentration leading to a non-uniform dispersion of CNCs within the PEEK. High concentrations of CNCs have shown to forms aggregates resulting in the CNCs interacting primarily with themselves instead of with the polymer matrix. With no clear trend to help explain the reinforcement of CNCs, the effect of the additive to the PEEK composite cannot be confirmed. The plasticization from remaining solvent could be more significant than the CNCs itself. At the same time, developing a consistent process for full removal of remaining solvent could reveal a trend of changing modulus with changing CNC content. With PEEK's modulus being 3 GPa and CNCs' modulus being 100-200 GPa developing a composite of the two materials should have produced a material with a young's modulus between 3 and 200 GPa. [12, 24] The introduction of CNCs to the composite could have been an introduction of voids thus lowering the density. Studies conducted have shown that there is a linear correlation of density and young's modulus for PEEK samples. [84] One aspect which was not replicated in the composite was the fiber orientation seen in human cortical bone. Collagen fibers align themselves in the direction of load correlating to the high strength properties in the longitudinal direction of human bone.

3.2.5 Compression Data

In compression, the PEEK composites showed variance in mechanical properties based on the drying temperature, but no clear trend with changes in CNC content. Samples dried at ambient-conditions displayed a plasticizing effect during the tests. Shown in Figure (28), ambient-dried samples flattened with no signs of crack propagation. Drying at 120 °C exhibited brittle fracture. From the compression data seen in Figure (29) and Table 2, the higher drying temperature increased the modulus by removing the remaining solvent that was acting as a plasticizer. This is illustrated in the PEEK samples dried at ambient conditions, 25 °C, and at 50 °C, the modulus increased from 53MPa to 180MPa with a slight increase in yield strength as well. Although having a higher concentration of CNCs, the 10wt% CNC composite did not show an increase in modulus. At 20wt% CNC, the modulus increased when compared to pure PEEK. Without statistical analysis,

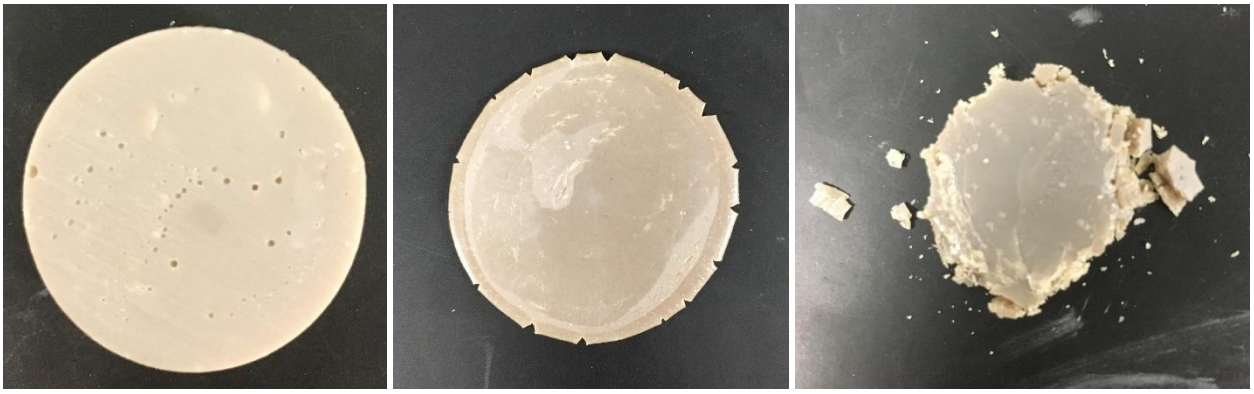

Figure 28: PEEK compression samples left) ambient-dried before testing, middle) ambient-dried after testing, right) 120 °C dried after testing

it is difficult to confirm if the 10wt% CNC had a lower modulus value, or if the 20wt% CNC had a higher modulus value. What can be confirmed is the effect of drying temperature on the mechanical properties. The 5wt% CNC samples were dried at 120 °C, in order to replicate the drying conditions of the DSC samples. The modulus increased greatly to 695MPa compared to the pure PEEK samples. With pure PEEK samples displaying an increase in modulus with an increase in drying temperature, it can be said that the removal of solvent based on drying increases the

*Table 2: Mechanical data of PEEK/CNC composites in compression. * indicating sample size of one*

CNC Weight Percent	Drying Temperature	Young's Modulus, MPa	Elongation at Break, %	Yield Strength, MPa
0	25 °C	53.0 ± 8.6	0.836 ± 0.02	115 ± 2.5
0	50 °C	180 ± 15	0.706 ± 0.01	157 ± 1.1
5	120 °C	695 ± 72	0.447 ± .08	137 ± 25
10	25 °C	41*	0.824*	108*
20	25 °C	372*	0.600*	160*

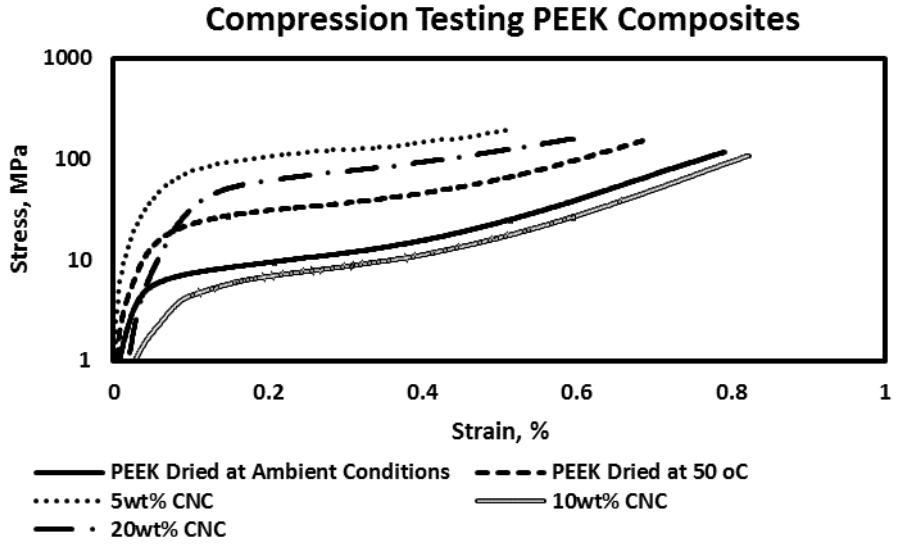

Figure 29: Stress vs. strain plots of PEEK/CNC composites in compression

modulus of the composite. However, the significance of the drying temperature in respect to the CNC content cannot be confirmed without a 5wt% CNC samples dried at ambient conditions. Similar to the tensile tests, the compression samples should be dried at the same temperature to investigate the correlation of the modulus changes with drying temperature changes. This would highlight the significance of the remaining solvent to the mechanical properties of the PEEK composites. Overall, the compression data displayed a small trend of increasing modulus with increasing drying temperature which can be contributed to the removal of entrapped solvent in the PEEK matrix.

4 Conclusion

PEEK can be solvent casted using chlorophenol as the main solvent. A solvent exchange process with ethanol can produce a material that was stiff enough for handling. Scanning electron microscopy uncovered varying structures of the PEEK depending on the drying method. When freeze-dried, the structure is porous with average pore sizes in the nanometer range, but these pores do not show up when the samples are left to dry at ambient conditions. Thermal analysis showed that the degradation point of PEEK is not altered from the solvent casting process besides drying at 120 °C causing an introduction of contaminants. DSC scans revealed signs of plasticizer due to residual solvents with a broad peak near the T_g as well as shifts in the crystallization temperature and crystallization enthalpies. However, by drying at 120 °C, DSC scans displayed a lesser degree of plasticization with the broad peak diminishing and the crystallization behavior in line with the PEEK powder. Mechanical testing of CNC/PEEK composites measured modulus values out of range of human bone. The additions of CNCs to the PEEK matrix had varying effects on the composites. In tension, at 10wt% CNC, the modulus increased but not the yield strength. 5 and 20wt% CNC displayed a lowering of the modulus and strength with an increase in elongation. With samples dried at ambient conditions, the hydrophilic CNCs withheld solvent leading to a lowering of mechanical properties. Additionally, the CNCs and the solvent casting process may introduce voids leading to a lowering in density that can help explain the low modulus values. A series of compression tests with samples prepared at varying drying conditions proved that the residual solvent was plasticizing the composites. The effect of CNC content on the composites could not be confirmed without statistical analysis and samples dried at the same temperature. Fortunately, drying temperature was shown to influence the modulus of the PEEK in compression

with an increase from 50 to 150MPa with a 25 °C increase in drying temperature. These findings suggest that PEEK can be solvent casted with the addition of organic and inorganic additives with structural changes based on the drying method, but the composites' mechanical properties were not in range of bone.

5 Future Work

A multitude of experiments can be performed to further correlate the process, structure and properties of the PEEK composites. For the structure of the PEEK composites, an investigation can be done on multiple solvents to see if the solvent's vapor pressure or miscibility with ethanol has an effect on the porosity and drying behavior of the composite. Additionally, SEM imaging on the samples dried at 120 °C should be done to look for further pore size differences. The increased temperature of drying could be promoting crystallization or compacting the PEEK as well as removing the solvent to increase the modulus. BET measurements can be performed to get quantitative data on the surface area and porosity of the PEEK. These measurements can be used to show if the porosity is altered with varying amounts of the CNCs and HA.

For thermal properties, the steady degradation of PEEK dried at 120 °C needs to be investigated. It needs to be determined if the initial degradation is caused by contamination during the drying process. If there is no evidence of contamination, then the next steps would be to do chemical analysis to look for possible changes in the chemistry of PEEK through FTIR and NMR.

For the mechanical properties, the composites should be dried at the same conditions with replicates for statistical analysis. For compression and tensile samples, drying at 120 °C should be carried out for all different compositions of CNC. Additionally, mechanical testing of HA composites is another next step to determine the effect of HA on the PEEK. It would be promising if the HA could increase the modulus of the PEEK enough to be in range of bone because of HA being a fuel source for bone growth. This would lead to the HA particles acting as the pores. Lastly, with HA/PEEK composites, bone growth studies can be done to show integration of bone cells in the composites.

References

1. Zhang, L.; He, Z. Y.; Zhang, Y. Q.; Jiang, Y. H.; Zhou, R., Rapidly sintering of interconnected porous Ti-HA biocomposite with high strength and enhanced bioactivity. *Materials Science and Engineering: C* **2016,** *67*, 104-114.
2. Dannhauer, M.; Lanfer, B.; Wolters, C. H.; Kn; ouml; sche, T. R., Modeling of the human skull in EEG source analysis. *Human Brain Mapping* **2011,** *32* (9), 1383-1399.
3. Nganga, S.; Zhang, D.; Moritz, N.; Vallittu, P. K., Multi-layer porous fiber-reinforced composites for implants: In vitro calcium phosphate formation in the presence of bioactive glass. *Dental Materials* **2012,** *28* (11), 1134-1145.
4. Nordqvist, C. Osteoarthritis: Causes, Symptomes and Treatments. **2017**
5. In *Bone Anatomy Cortex Cortical Bone And Cancellous Bone Bone And Spine*, AnatomyLibrary99, **2016**.
6. Britannica, Osteocyte. *Encyclopædia Britannica*, Encyclopædia Britannica, inc.: **2015**.
7. Sugerman, D.; Deborah Tolmach, S., Osteoporosis. *JAMA : The Journal of the American Medical Association* **2014,** *311* (1), 104.
8. Pal, S., Mechanical Properties of Biological Materials. *Design of Artificial Human Joints & Organs*, Springer US: Boston, MA, **2014**; pp 23-40.
9. Ryan, G.; Ryan, G.; Pandit, A.; Apatsidis, D. P., Fabrication methods of porous metals for use in orthopaedic applications. *Biomaterials* **2006,** *27* (13), 2651-2670.
10. Roos, E., Joint injury causes knee osteoarthritis in young adults. *Current Opinion in Rheumatology* **2005,** *17* (2), 195.
11. de l'Escalopier, N.; Anract, P.; Biau, D., Surgical treatments for osteoarthritis. *Annals of Physical and Rehabilitation Medicine* **2016,** *59* (3), 227-233.
12. Abu Bakar, M. S.; Abu Bakar, M. S.; Cheng, M. H. W.; Tang, S. M.; Yu, S. C., Tensile properties, tension–tension fatigue and biological response of polyetheretherketone–hydroxyapatite composites for load-bearing orthopedic implants. *Biomaterials* **2003,** *24* (13), 2245-2250.
13. Lim, K. L. K.; Lim, K. L. K.; Ishak, Z. A. M.; Ishiaku, U. S.; Fuad, A. M. Y., High density polyethylene/ultra high molecular weight polyethylene blend. II. Effect of hydroxyapatite on processing, thermal, and mechanical properties. *Journal of Applied Polymer Science* **2015,** *100* (5), 3931-3942.
14. Torstrick, F. B.; Evans, N. T.; Stevens, H. Y.; Gall, K.; Guldberg, R. E., Do Surface Porosity and Pore Size Influence Mechanical Properties and Cellular Response to PEEK? *Clinical Orthopaedics and Related Research®* **2016,** *474* (11), 2373-2383.
15. Kurtz, S.; Ong, K.; Lau, E.; Mowat, F.; Halpern, M., Projections of Primary and Revision Hip and Knee Arthroplasty in the United States from 2005 to 2030. *JBJS* **2007,** *89* (4), 780-785.
16. Paschos, N. K., Anterior cruciate ligament reconstruction and knee osteoarthritis. *World Journal of Orthopedics* **2017,** *8* (3), 212-217.
17. Thomas, P., Clinical and diagnostic challenges of metal implant allergy using the example of orthopaedic surgical implants: Part 15 of the Series Molecular Allergology. *Allergo Journal International* **2014,** *23* (6), 179-185.

18. Wengler, A.; Nimptsch, U.; Mansky, T., Hip and Knee Replacement in Germany and the USA: Analysis of Individual Inpatient Data From German and US Hospitals for the Years 2005 to 2011. *Deutsches Ärzteblatt International* **2014,** *111* (23-24), 407-416.
19. Arifin, A.; Sulong, A. B.; Muhamad, N.; Syarif, J.; Ramli, M. I., Material processing of hydroxyapatite and titanium alloy (HA/Ti) composite as implant materials using powder metallurgy: A review. *Materials & Design* **2014,** *55*, 165-175.
20. Currey, J. D., *Bones : Structure and Mechanics (2)*. Princeton University Press: Princeton, US, **2013**.
21. Ma, R.; Tang, T., Current Strategies to Improve the Bioactivity of PEEK. *International Journal of Molecular Sciences* **2014,** *15* (4), 5426-5445.
22. Panayotov, I. V.; Orti, V.; Cuisinier, F.; Yachouh, J., Polyetheretherketone (PEEK) for medical applications. *Journal of Materials Science: Materials in Medicine* **2016,** *27* (7), 118.
23. Tan, K. H.; Chua, C. K.; Leong, K. F.; Cheah, C. M.; Cheang, P.; Abu Bakar, M. S.; Cha, S. W., Scaffold development using selective laser sintering of polyetheretherketone–hydroxyapatite biocomposite blends. *Biomaterials* **2003,** *24* (18), 3115-3123.
24. Lin, N.; Dufresne, A., Nanocellulose in biomedicine: Current status and future prospect. *European Polymer Journal* **2014,** *59*, 302-325.
25. Jorfi, M.; Foster, E. J., Recent advances in nanocellulose for biomedical applications. *Journal of Applied Polymer Science* **2015,** *132* (14), n/a-n/a.
26. Passantino, J. M.; Passantino, J. M.; Haywood, A. D.; Goswami, J.; Davis, V. A., Effects of Polymer Additives and Dispersion State on the Mechanical Properties of Cellulose Nanocrystal Films. *Macromolecular Materials and Engineering* **2017,** *302* (4), 1600351.
27. Fricain, J. C.; Fricain, J. C.; Granja, P. L.; Barbosa, M. A.; de, J.; eacute; so, B., Cellulose phosphates as biomaterials. In vivo biocompatibility studies. *Biomaterials* **2002,** *23* (4), 971-980.
28. Houliara, S.; Karamanos, S. A., Buckling of Thin-Walled Long Steel Cylinders Subjected to Bending. *Journal of Pressure Vessel Technology* **2011,** *133* (1), 11201.
29. Colnot, C.; Zhang, X.; Tate, M. L. K., Current insights on the regenerative potential of the periosteum: Molecular, cellular, and endogenous engineering approaches. *Journal of Orthopaedic Research* **2012,** *30* (12), 1869-1878.
30. Evans, S. F.; Parent, J. B.; Lasko, C. E.; Zhen, X.; Knothe, U. R.; Lemaire, T.; Knothe Tate, M. L., Periosteum, bone's "smart" bounding membrane, exhibits direction-dependent permeability. *Journal of Bone and Mineral Research* **2013,** *28* (3), 608-617.
31. Eriksen, E. F., Cellular mechanisms of bone remodeling. *Reviews in Endocrine and Metabolic Disorders* **2010,** *11* (4), 219-227.
32. Naili, S.; Naili, S.; van Rietbergen, B.; Sansalone, V.; Taylor, D., Bone remodeling. *Journal of the Mechanical Behavior of Biomedical Materials* **2011,** *4* (6), 827-828.
33. van der Kraan, P. M.; van den Berg, W. B., Osteophytes: relevance and biology. *Osteoarthritis and Cartilage* **2007,** *15* (3), 237-244.
34. Bala, Y.; Zebaze, R.; Seeman, E., Role of cortical bone in bone fragility. *Current Opinion in Rheumatology* **2015,** *27* (4), 406-413.
35. Cooper, D. M. L.; Kawalilak, C. E.; Harrison, K.; Johnston, B. D.; Johnston, J. D., Cortical Bone Porosity: What Is It, Why Is It Important, and How Can We Detect It? *Current Osteoporosis Reports* **2016,** *14* (5), 187-198.
36. Racila, M.; Crolet, J. M., Nano and Macro Structure of Cortical Bone: Numerical Investigations. *Mechanics of Advanced Materials and Structures* **2007,** *14* (8), 655-663.

37. Libonati, F.; Vergani, L., Understanding the structure–property relationship in cortical bone to design a biomimetic composite. *Composite Structures* **2016,** *139*, 188-198.
38. Clarke, B., Normal Bone Anatomy and Physiology. *Clinical Journal of the American Society of Nephrology* **2008,** *3* (Supplement 3), S131-S139.
39. Murugan, R.; Murugan, R.; Ramakrishna, S., Development of nanocomposites for bone grafting. *Composites science and technology* **2005,** *65* (15), 2385-2406.
40. Neil Dong, X.; Edward Guo, X., The dependence of transversely isotropic elasticity of human femoral cortical bone on porosity. *Journal of Biomechanics* **2004,** *37* (8), 1281-1287.
41. Havaldar, R.; Pilli, S. C.; Putti, B. B., Insights into the effects of tensile and compressive loadings on human femur bone. *Advanced Biomedical Research* **2014,** *3*, 101.
42. Goldring, M. B.; Goldring, M. B.; Goldring, S. R., Osteoarthritis. *Journal of Cellular Physiology* **2007,** *213* (3), 626-634.
43. Reginster, J.-Y.; Neuprez, A.; Lecart, M.-P.; Sarlet, N.; Bruyere, O., Role of glucosamine in the treatment for osteoarthritis. *Rheumatology International* **2012,** *32* (10), 2959-2967.
44. Vaquero, J.; Forriol, F., Meniscus tear surgery and meniscus replacement. *Muscles, Ligaments and Tendons Journal* **2016,** *6* (1), 71-89.
45. Koonce, R. C.; Bravman, J. T., Obesity and Osteoarthritis: More Than Just Wear and Tear. *Journal of the American Academy of Orthopaedic Surgeons* **2013,** *21* (3), 161-169.
46. Brakke, R.; Singh, J.; Sullivan, W., Physical Therapy in Persons With Osteoarthritis. *PM & R* **2012,** *4* (5), S53-S58.
47. Segal, N. A.; Findlay, C.; Wang, K.; Torner, J. C.; Nevitt, M. C., The longitudinal relationship between thigh muscle mass and the development of knee osteoarthritis. *Osteoarthritis and Cartilage* **2012,** *20* (12), 1534-1540.
48. Wolff law. In *Stedman's Medical Dictionary for the Health Professions and Nursing*, Wolters Kluwer Health, Lippincott Williams & Wilkins: **2012**.
49. Chen, J.-H.; Liu, C.; You, L.; Simmons, C. A., Boning up on Wolff's Law: Mechanical regulation of the cells that make and maintain bone. *Journal of Biomechanics* **2010,** *43* (1), 108-118.
50. Shirazi, R.; Shirazi, A., Role of cartilage collagen fibrils networks in knee joint biomechanics under compression. *Journal of Biomechanics* **2008,** *41* (16), 3340-3348.
51. Nunez, M.; Nunez, E.; Lozano, L.; Sastre, S.; Segur, J. M., Quality of life after joint replacement for osteoarthritis. *Aging Health* **2010,** *6*, 481+.
52. Hurtig, M.; Chubinskaya, S.; Dickey, J.; Rueger, D., BMP-7 protects against progression of cartilage degeneration after impact injury. *Journal of Orthopaedic Research* **2009,** *27* (5), 602-611.
53. Badlani, N.; Neil, B.; Yasushi, O.; Rob, H.; Richard, C., Use of Bone Morphogenic Protein-7 as a Treatment for Osteoarthritis. *Clinical Orthopaedics and Related Research* **2009,** *467* (12), 3221-3229.
54. Ebeling , P. R., Osteoporosis in Men. *New England Journal of Medicine* **2008,** *358* (14), 1474-1482.
55. Dupree, K.; Dobs, A., Osteopenia and Male Hypogonadism. *Reviews in Urology* **2004,** *6* (Suppl 6), S30-S34.
56. Vitamin D and bone growth - Scientific substantiation of a health claim related to vitamin D and bone growth pursuant to Article 14 of Regulation (EC) No 1924/2006 - Scientific Opinion of the Panel on Dietetic Products, Nutrition and Allergies. *EFSA Journal* **2008,** *6* (10), 827-n/a.

57. Duckham, R. L.; Rantalainen, T.; Ducher, G.; Hill, B.; Telford, R. D.; Telford, R. M.; Daly, R. M., Effects of Habitual Physical Activity and Fitness on Tibial Cortical Bone Mass, Structure and Mass Distribution in Pre-pubertal Boys and Girls: The Look Study. *Calcified Tissue International* **2016,** *99* (1), 56-65.
58. Wu, D.; Li, X.; Tao, C.; Dai, R., Association of microstructural and mechanical properties of cancellous bone and their fracture risk assessment tool scores. *International Journal of Clinical and Experimental Medicine* **2015,** *8* (3), 3956-3964.
59. Chen, H.; Zhou, X.; Fujita, H.; Onozuka, M.; Kubo, K.-Y., Age-Related Changes in Trabecular and Cortical Bone Microstructure. *International Journal of Endocrinology* **2013,** *2013*, 9.
60. Eriksen, E. F.; Halse, J.; Moen, M. H., New developments in the treatment of osteoporosis. *Acta Obstetricia et Gynecologica Scandinavica* **2013,** *92* (6), 620-636.
61. Eriksen, E. F.; Melsen, F.; Sod, E.; Barton, I.; Chines, A., Effects of long-term risedronate on bone quality and bone turnover in women with postmenopausal osteoporosis. *Bone* **2002,** *31* (5), 620-625.
62. Russell, R. G. G.; Watts, N. B.; Ebetino, F. H.; Rogers, M. J., Mechanisms of action of bisphosphonates: similarities and differences and their potential influence on clinical efficacy. *Osteoporosis International* **2008,** *19* (6), 733-759.
63. Bischoff-Ferrari, H. A.; Can, U.; Staehelin, H. B.; Platz, A.; Henschkowski, J.; Michel, B. A.; Dawson-Hughes, B.; Theiler, R., Severe vitamin D deficiency in Swiss hip fracture patients. *Bone* **2008,** *42* (3), 597-602.
64. Sinaki, M.; Pfeifer, M.; Preisinger, E.; Itoi, E.; Rizzoli, R.; Boonen, S.; Geusens, P.; Minne, H. W., The Role of Exercise in the Treatment of Osteoporosis. *Current Osteoporosis Reports* **2010,** *8* (3), 138-144.
65. Hurley, B.; Armstrong, T. J., Bisphosphonates vs Exercise for the Prevention and Treatment of Osteoporosis. *Journal for Nurse Practitioners* **2012,** *8* (3), 217-224.
66. Braith, R. W.; Magyari, P. M.; Fulton, M. N.; Aranda, J.; Walker, T.; Hill, J. A., Resistance exercise training and alendronate reverse Glucocorticoid-Induced osteoporosis in heart transplant recipients. *The Journal of Heart and Lung Transplantation* **2003,** *22* (10), 1082-1090.
67. Wegener, B., Microstructure, cytotoxicity and corrosion of powder-metallurgical iron alloys for biodegradable bone replacement materials. *Materials Science & Engineering. B, Solid-State Materials for Advanced Technology* **2011,** *176* (20), 1789-1796.
68. Lefebvre, L. P.; Banhart, J.; Dunand, D. C., Porous Metals and Metallic Foams: Current Status and Recent Developments. *Advanced Engineering Materials* **2008,** *10* (9), 775-787.
69. Seah, K. H. W.; Thampuran, R.; Teoh, S. H., The influence of pore morphology on corrosion. *Corrosion Science* **1998,** *40* (4), 547-556.
70. Anawati, H.; Anawati; Tanigawa, H.; Asoh, H.; Ohno, T., Electrochemical corrosion and bioactivity of titanium-hydroxyapatite composites prepared by spark plasma sintering. *Corrosion Science* **2013,** *70*, 212-220.
71. Martin, R. I.; Brown, P. W., Mechanical properties of hydroxyapatite formed at physiological temperature. *Journal of Materials Science: Materials in Medicine* **1995,** *6* (3), 138-143.
72. Wagoner Johnson, A. J.; Herschler, B. A., A review of the mechanical behavior of CaP and CaP/polymer composites for applications in bone replacement and repair. *Acta Biomaterialia* **2011,** *7* (1), 16-30.

73. Zhang, Y.; Tanner, K. E.; Gurav, N.; Di Silvio, L., In vitro osteoblastic response to 30 vol% hydroxyapatite-polyethylene composite. *Journal of Biomedical Materials Research Part A* **2007,** *81A* (2), 409-417.
74. Zhang, Y.; Tanner, K. E., Impact behavior of hydroxyapatite reinforced polyethylene composites. *Journal of Materials Science: Materials in Medicine* **2003,** *14* (1), 63-68.
75. Fink, J. K., Chapter 6 - Poly(aryl ether ketone)s. *High Performance Polymers (Second Edition)*, William Andrew Publishing: **2014**; pp 153-175.
76. Xu, J.; Zhang, Z.; Xiong, X.; Zeng, H., A new solvent for poly(ether ether ketone). *Polymer*, **1992**; Vol. 33, pp 4432-4434.
77. Sonpingkam, S.; Pattavarakorn, D., *Mechanical Properties of Sulfonated Poly (Ether Ether Ketone) Nanocomposite Membranes*. **2014**; Vol. 5, p 181-185.
78. Scholes, S. C.; Unsworth, A., Wear studies on the likely performance of CFR-PEEK/CoCrMo for use as artificial joint bearing materials. *Journal of Materials Science: Materials in Medicine* **2008,** *20* (1), 163.
79. Scherer, G. W., Theory of Drying. *Journal of the American Ceramic Society* **1990,** *73* (1), 3-14.
80. Mishra, T. K.; Mishra, T. K.; Kumar, A.; Verma, V.; Pandey, K. N., PEEK composites reinforced with zirconia nanofiller. *Composites Science and Technology* **2012,** *72* (13), 1627-1631.
81. Patel, P.; Hull, T. R.; McCabe, R. W.; Flath, D.; Grasmeder, J.; Percy, M., Mechanism of thermal decomposition of poly(ether ether ketone) (PEEK) from a review of decomposition studies. *Polymer Degradation and Stability* **2010,** *95* (5), 709-718.
82. Lu, P.; Hsieh, Y.-L., Preparation and properties of cellulose nanocrystals: Rods, spheres, and network. *Carbohydrate Polymers* **2010,** *82* (2), 329-336.
83. Liao, C.-J.; Lin, F.-H.; Chen, K.-S.; Sun, J.-S., Thermal decomposition and reconstitution of hydroxyapatite in air atmosphere. *Biomaterials* **1999,** *20* (19), 1807-1813.
84. Talley, S. J.; Yuan, X.; Moore, R. B., Thermoreversible Gelation of Poly(ether ether ketone). *ACS Macro Letters* **2017,** *6* (3), 262-266.